Differential Reflectivity Calibration for NEXRAD

FY2007 Interim Report

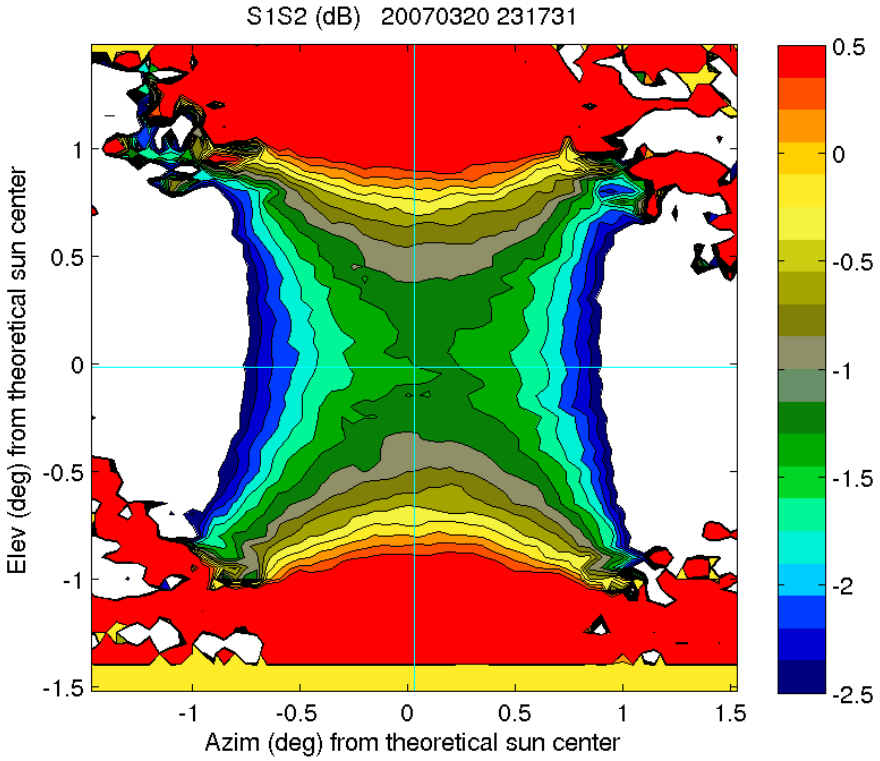

The S_1S_2 S-Pol solar antenna pattern

Prepared for:
NEXRAD Product Improvement Program
NWS, Office of Science and Technology

By: J.C. Hubbert, F. Pratte, M. Dixon and R. Rilling

National Center for Atmospheric Research

15 June 2007

Contents

Executive Summary

NCAR (National Center for Atmospheric Research) has been tasked by the NOAA/NWS Office of Science and Technology to investigate, test and quantify the uncertainty of several techniques to calibrate differential reflectivity (Z_{dr}) for the future dual polarized NEXRADs using S-Pol, NCAR's S-band polarimetric radar, as a test bed. Z_{dr} is the ratio of copolar horizontal to copolar vertical reflectivities.

The most widely accepted way to calibrate Z_{dr} is the vertical pointing (VP) method. Data is gathered while the radar dish is pointing vertically in light rain and such data provides an external measure of near-zero Z_{dr} (Bringi and Chandrasekar 2001). The NEXRAD radars are physically incapable of pointing vertically (60° is the maximum elevation angle) and therefore cannot use this method for Z_{dr} calibration. However, S-Pol can point vertically and such vertical pointing Z_{dr} measurements are used as a calibration reference in the evaluation of other Z_{dr} calibration techniques. The Z_{dr} bias statistics calculated via the vertical pointing technique are evaluated in this report and it is shown that the uncertainty of the VP Z_{dr} bias estimate is well with in the desired 0.1 dB level.

A main thrust of NCAR's Z_{dr} calibration project is to determine the viability of the NSSL-proposed engineering calibration (EC) proposal (Zrnić et al. 2006) and to evaluate the uncertainty of the method. The EC technique is based on a combination of differential gain measurements of considered static portions of the horizontal (H) and vertical (V) paths (e.g., waveguides and antenna) plus on-line monitoring/correction of the active paths (i.e., the receiver). The EC method uses solar flux reception to obtain differential receiver path gain. The EC technique also requires several differential waveguide power measurements which are difficult to accomplish within a 0.1 dB uncertainty. Using manufacture uncertainty specifications for some typical high quality measurement equipment and knowledge of typical impedance mismatch values, waveguide absolute power measurements as well as differential power measurements have a theoretical estimated combined expanded uncertainty of about 0.20 dB. Again, this is for excellent test equipment that is well calibrated and for an experienced, meticulous technician(expanded uncertainty denote 2σ coverage or a 95% confidence interval). Even though the differential power measurement has several uncertainty terms cancel, there is the additional uncertainty of the extra waveguide coupling factor that dominates the uncertainty budget. Even if instrumentation corrections are made (e.g., precise impedance mismatch factors can be measured and corrected in a calibration laboratory), the these two uncertainty numbers may be reduced to about 0.12 dB, at least theoretically. However,such an approached to the operation calibration of Z_{dr} for the NEXRADs would like be cost prohibitive and practically difficult to execute. It is shown that by using a combination of Type A evaluations (repeated measurements) and Type B evaluations (e.g.,manufacturer specifications), the uncertainty of the NSSL EC technique is about 0.30 dB. If measurement methods are improved, this uncertainty is likely to be reduced somewhat.

To evaluate the EC method rigorously, repeated connect and disconnects of RF equipment need to be eliminated and, in general, any human interface variability also needs to be reduced to a minimum. To accomplish this, a network of RF test equipment for automated measurements has been assembled that will be used to reduce the uncertainty of RF power measurements and thereby improve the evaluation of the EC technique. The network of RF measurement equipment is referred to as the Automated Test Equipment system (ATE) which has been constructed and the accompanying Labview control software is now nearly completed.

Recently, NSSL has proposed an abbreviated EC technique that reduces the number of required power

measurements. Also, NCAR has designed an abbreviated EC technique. Both techniques are evaluated in this report. Uncertainty budget analysis of the three EC techniques show that the NCAR abbreviated method has the smallest uncertainty, though marginally, which is about 0.25 dB.

Also evaluated is the crosspolar power (CP) calibration technique that only uses passive sun measurements and crosspolar power measurements to estimate the system Z_{dr} bias. By not relying on any obtrusive RF power measurements, the uncertainty introduced by such measurements is avoided. S-Pol measurements thus far support the viability and validity of this technique. The uncertainty of this method is evaluated, via S-Pol experimental data, to be less than 0.1 dB. The calculated CP Z_{dr} bias agrees very well with the calculated Z_{dr} bias from vertical pointing data. It is also shown via experimental data that the CP technique can be accomplished using alternating PPI scans of transmit H polarization and then V polarization, using ground clutter targets, thus making the CP technique a viable alternative for Z_{dr} calibration on NEXRAD. Further statistical evaluation is needed, however.

Both the EC and CP techniques rely on sun measurements. It is shown that the uncertainty of mean sun power measurement ratios can be measured to within 0.1 dB. Also, pseudo antenna patterns are calculated from sun scan data so that the horizontal and vertical antenna pattern mismatch can be evaluated, at least over the main antenna beam. Well matched H and V antenna patterns are required if Z_{dr} biases are to be avoided in regions of high reflectivity gradient.

It is emphasized that the following results are still preliminary and need to be further investigated, quantified and verified via more data collection and analysis.

1 INTRODUCTION

NCAR (National Center for Atmospheric Research) has been tasked by the NWS (National Weather Service) to determine the uncertainty of various methods for the calibration of Z_{dr} using S-Pol, NCAR's S-band polarimetric radar. Three techniques are investigated 1) the vertical pointing (VP) technique, 2) the engineering calibration (EC) technique and 3) the crosspolar power (CP) technique. A primary focus of this report is to define the "goodness" of the experimentally determined Z_{dr} biases or calibration factors found from each technique. However, estimating Z_{dr} errors from known manufacture specifications and knowledge of RF (radio frequency) measurement test equipment topology (e.g., impedance mismatches) is also of central importance. Uncertainty of measurements is a way to quantify the probability that a measurement(in the present case a calculated calibration factor) lies within some error bounds. For clarity, uncertainty and the related measurement techniques and quantities used in this report are defined in Section 2.

The most widely accepted way to calibrate Z_{dr} is the VP method and this technique is used as a calibration reference by which to evaluate the other two techniques. Since the orientation distribution of precipitation particles when viewed vertically in the plane of polarization is uniformly random, the intrinsic value of Z_{dr} is 0 dB for such scatterers. Thus, data gathered while the radar antenna is pointing vertically in light rain provides an external measure of nearly zero dB Z_{dr} (Bringi and Chandrasekar 2001). Histograms of Z_{dr} from such VP data have intrinsic average values of 0 dB and this is how Z_{dr} for S-Pol and other research radars has been calibrated in the past. Unfortunately, the NEXRADs cannot point vertically and therefore cannot use the VP approach for Z_{dr} calibration.

A second way to calibrate Z_{dr} is with an EC approach based on engineering measurements and the following instrument model (Zrnić et al. 2006). The radar transmit and receive paths are divided into "active" and "passive" parts. The gains and losses of the "passive" or "static" parts, i.e. the waveguides and antenna, are measured by using test signals and radiation from the sun. The gain of the active signal path (i.e., receiver chain) is monitored via test signal injection on a continuous basis. Transmit powers are also monitored. By combining the passive and active calibration measurements, the Z_{dr} bias can be estimated. The uncertainty of the EC approach is estimated from a combination of prior experience (Type B evaluation; e.g., manufacturer uncertainty specifications) and on repeated measurements (Type A evaluation) (Taylor and Kuyatt, 1994). Type A evaluations of RF power measurement uncertainty can typically be quite small if the repeated power measurements of a signal with the same measurement equipment is executed by the same technician over a brief time interval, (say minutes). *We show that Type B uncertainty is dominant in the uncertainty budgets of the evaluated EC calibration techniques*.

A third method for Z_{dr} calibration makes use of the principle of radar reciprocity which states that the two crosspolar members of the radar scattering matrix are equal, i.e, $S_{hv} = S_{vh}$ (Saxon, 1955). Practically, this means that the crosspolar powers measured with a fast alternating H-V polarization transmit radar are equal if the H and V transmit powers are equal. Use of this fact along with passive sun measurements can be used to calibrate Z_{dr} and this technique is termed the crosspolar power (CP) approach for Z_{dr} calibration. The CP method is not based on isotropy of the scatterers (as is the VP method) exact and has been demonstrated previously with CSU-CHILL radar data (Hubbert et al. 2003). Operationally, the NEXRADs will transmit H and V polarization simultaneously and thus this method will not work directly as it has on S-Pol and CSU-CHILL, i.e., near simultaneous samples of the two crosspolar powers are not available as is the case for fast H and V alternating polarization transmission. However, the average crosspolar powers from stationary ground clutter targets (e.g., from consecutive PPI surveillance scans at H and V polarization if indexed beams are used) can be measured by employing a slow mechanical switch to alternate H and V transmit polarizations. This will be accomplished since the backscatter cross sections

of stationary ground clutter targets are invariant (ground clutter targets such as trees that can move with the wind are exceptions). This has not been previously demonstrated but is shown in this report with S-Pol data.

Uncertainty budgets of the three Z_{dr} calibration approaches are compared and discussed. The NCAR Z_{dr} calibration experiment is ongoing and we show preliminary results that indicate the uncertainty of each method using experimental data from NCAR's S-Pol. We emphasize that the uncertainty estimates reported herein are preliminary and larger data sets need to be gathered and analyzed.

2 UNCERTAINTY ANALYSIS

Calibration is a measurement process that assigns values to the property of an artifact or to the response of an instrument relative to reference standards or to a designated measurement process. Its purpose is to reduce the bias of the measurement process. There are measurement errors associated with this measurement process. Uncertainty can be defined as an estimate of the expected limits of experimental error. Uncertainty of measurement arises from incomplete knowledge, control, understanding, definition of the processes influencing the measurement. Influence effects, such as temperature, humidity, frequency, mechanical stresses, path variations, and mismatches affect the result of measurements. (See http://www.itl.nist.gov/div898/handbook/index.htm for more detailed treatment of calibration and uncertainty).

Uncertainty can be categorized as either Type A or Type B. Type A uncertainty is represented by the standard deviation of a set of measurements and is primarily quantified by repetition under controlled test conditions(sometimes referred to as under statistical control). Type B uncertainty can also be represented by the standard deviation of an assumed Normal Distribution but is not quantified through measurement. It is quantified through manufacture specifications and other prior knowledge.

Errors can also be categorized (modeled) as systematic or random. Systematic measurement errors bias the mean of a measurement data set, i.e., increasing the number of measurements and averaging will not reduce systematic error as it will random errors. One way to detect and correct for systematic errors is to use a calibration standard, if one exists. Typically, subtle systematic errors are the most difficult to detect, model and quantify. If all systematic errors are eliminated the remaining fluctuations in a measurement data set are considered random measurement errors and can be quantified by calculation of the standard deviation of the data set. The random errors are usually considered Gaussian distributed but this assumption should be examined for each data set. The systematic errors, however, can also be modeled as random Gaussian distributed and included in an uncertainty budget.

As an example of the above concepts, consider a RF waveguide coupler. It may be marked by the manufacturer as having -37 dB ± 0.3 dB coupling factor; that is, if 100 of these waveguide couplers were tested, the average coupling factor would be -37 dB and the distribution of the coupling factors would be Gaussian with a two standard deviation (σ) of 0.3 dB (a 2σ confidence interval is the typical industry standard). If this device is used for RF waveguide power measurements, no amount of repeated measurements will reveal the likely systematic error present. This is then a Type B uncertainty. One perhaps could take the coupler to a sophisticated calibration lab and ascertain that the coupling factor is more precisely -37.1dB +/- 0.05 dB and thus the Type B uncertainty is reduced and becomes a Type A uncertainty. After inserting the coupler into the radar system, the resulting measurement error will still be systematic but the uncertainty can be quantified with the ± 0.05 dB measured specification. Thus, all errors may be considered random variables.

An uncertainty specification is incomplete without a confidence interval (Taylor and Kuyatt 1994).

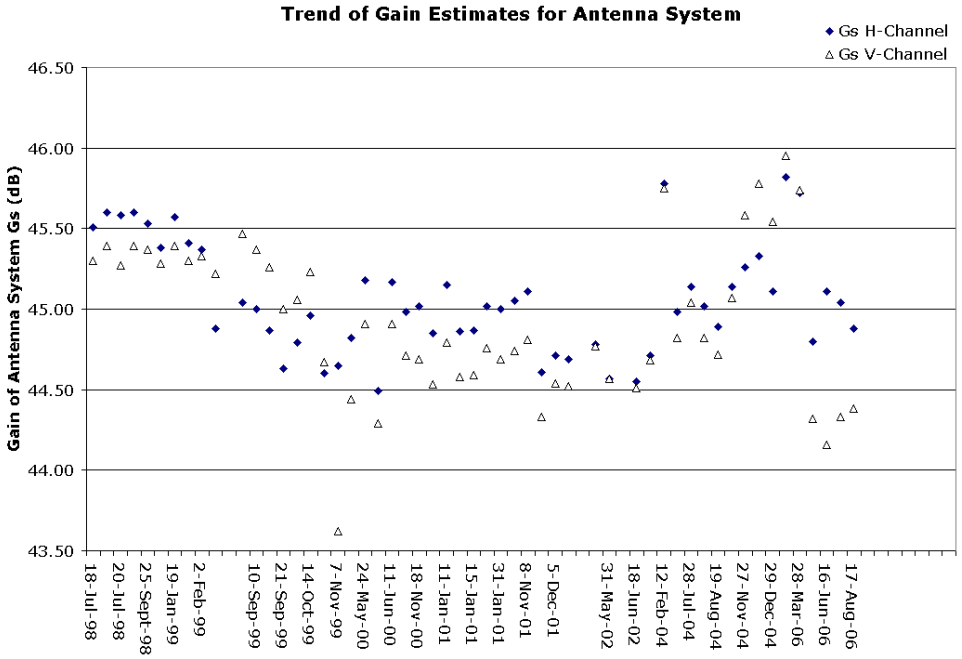

Figure 1: *S-Pol copolar antenna gain estimates from sun flux over 6 years.*

The confidence interval used in this report is 2σ or two standard deviations. This is sometimes referred to as 2σ coverage. The 2σ coverage standard is used in this report since this is the coverage value typically used by manufactures of RF devices. It also seems reasonable that meteorologist/hydrologists would like to use Z_{dr} measurements that are calibrated to within 0.1 dB with 95% confidence (i.e., 2σ coverage). In fact, the NEXRAD Technical Advisory Committee recently recommended (in March 2007) that Z_{dr} be calibrated to within 0.1 dB with 95% confidence (i.e., 2σ coverage). Thus, the measurements presented in this report are expressed as

$$E = M \pm \delta \tag{1}$$

where E is the quantity estimated, M is the measurement (or mean of measurements) and δ represents the uncertainty of the measurement with 2σ coverage. The desired Z_{dr} calibration goal can be expressed as

$$Z_{dr}^{cal} = Z_{dr}^{m} + Z_{dr}^{bias} \pm \delta \tag{2}$$

Where Z_{dr}^{cal} is the corrected or calibrated Z_{dr}, Z_{dr}^{m} is the measured Z_{dr} estimated from radar data, Z_{dr}^{bias} is the Z_{dr} bias calculated via one of the calibration techniques, and δ is the 2σ uncertainty of the bias estimate. For details on the calculation of uncertainty, see Appendix A.

Next, we give a measurement example of long term calibration measurements from S-Pol. Figure 1 provides as a realistic example of a long-term temporal trend of engineering measurements in S-Pol's antenna gain estimates. The estimates derived from sun flux measurements were made using essentially the same procedure over a period of eight years (1998-2006). Gain is measured from the reference plane coupler (see Fig. 5) through the antenna to the far field. It is a factor in the weather radar equation, its error combining with other errors. The evident temporal variation in Fig. 1 includes, at a minimum, changes in

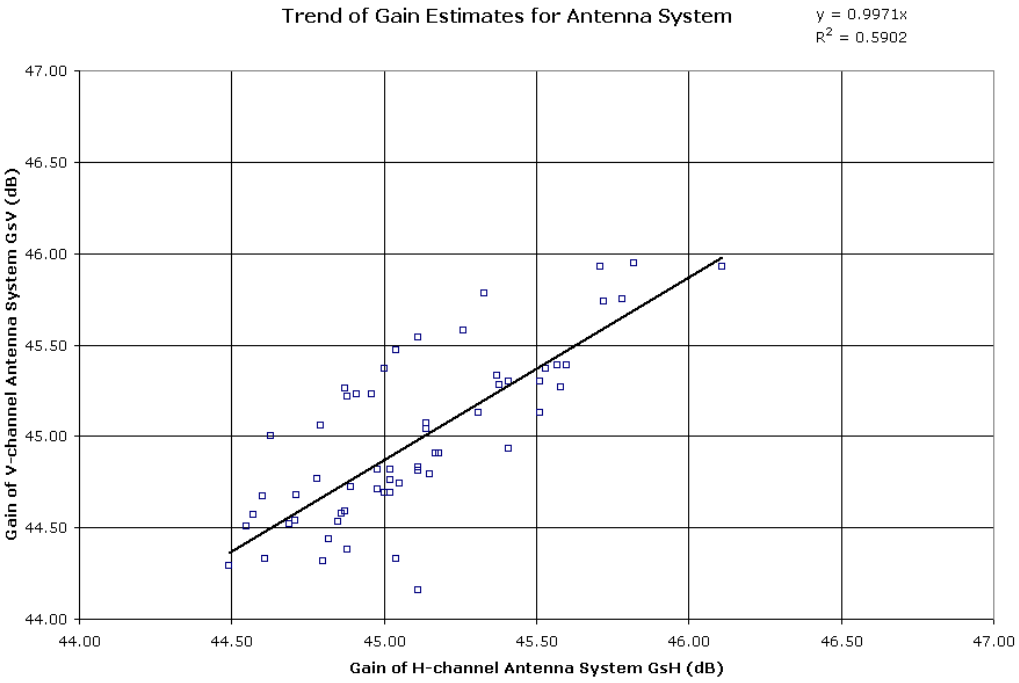

Figure 2: *Linear regression of S-Pol copolar V to H antenna gain estimates from sun flux over 8 years.*

true value from antenna reassembly and short-term measurement errors. Long-term bias effects are likely present but are hard to quantify at the tenths-of-decibel-level. The important aspect of error decomposition is difficult, especially without intermediate readings and redundant measurements. However, the results show that the overall standard deviation of the set of H-channel system gain estimates is roughly 0.36 dB, and that for the V-channel is 0.45 dB. Figure 2 show a linear regression of the V-channel estimates on the H-channel estimates and the standard deviation of the V-gain is found to be 0.29 dB. These estimates by themselves appear to bound the uncertainty but do not adequately portray the underlying accuracy of the parameter for a specific field experiment.

Use of automated test equipment, described later, for calibration measurements permits more complete decomposition of Z_{dr} uncertainty and will reduce human error and variance in measurement due to repeated connects and disconnects. Such equipment and methodology will improve the understanding of the measurement process and the quantification of the uncertainty. Whether or not the Z_{dr} calibration measurement uncertainty can be reduced to less than 0.1 dB is currently being evaluated using S-Pol as a test bed for NEXRAD.

3 ENGINEERING CALIBRATION APPROACH

The EC method breaks the calibration task into two parts: 1) measurement of the gain of the *static* portion of the of the signal path via injected signals, passive solar radiation and power meters, and 2) monitoring of the *dynamic* portion of the received signal path via the injection of test pulses. The static portions of the signal path are the waveguides and antenna. It is hypothesized that these signals can be measured accurately enough to calibrate Z_{dr} to within 0.1 dB uncertainty. The active or time varying portion of the receiver chain runs from the circulators through the I&Q digital samples. The active portion of the

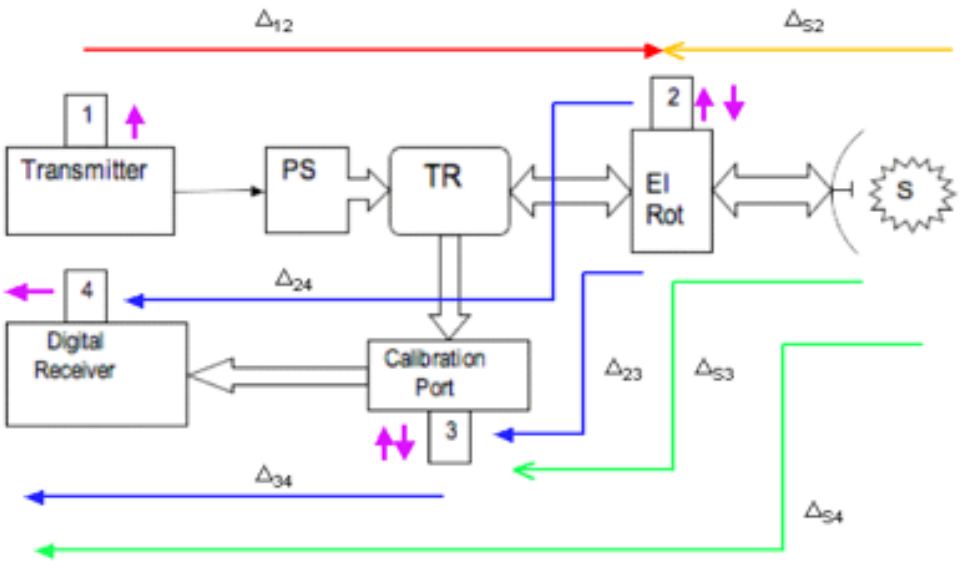

Figure 3: *A block diagram of a radar system for the EC method.*

receiver chain likely needs to be monitored on a volume scan to volume scan basis using test pulses.

3.1 *The NSSL Engineering Calibration Technique*

The NSSL EC method which has been tested on KOUN, NSSL's research radar, is described next (Zrnić et al. 2006). The method begins with an engineering calibration phase followed by an automatic built-in calibration-maintenance phase. The procedure attempts to separate the time-invariant factors from the drift factors. The time-invariant factors are measured once in the EC method to establish a constant correction valid for the radar's full dynamic range. The time varying factors are to be measured by an on-line calibration maintenance function based upon test signal injection. Figure 3 appears in NSSL's description of the EC method. A summary of the EC method is as follows: manually measure the differential transmit loss from point 1 to point 2, the differential receive loss from solar flux S to point 4, the differential receive loss from point 2 to point 4, and the differential receive loss from point 3 to point 4. Invoke reciprocity and calculate the differential transmit loss from point 1 to point S and calculate the differential receive loss from point S to point 3. Assume that like-path errors are highly correlated so they cancel, and assume the passive transmission factors remain constant to much better than 0.1 dB. The Z_{dr} bias calibration equation is

$$\begin{aligned} Z_{dr}^{bias} &= \Delta(1,2)_{pulse} + 2\left[\Delta(S,4)_{noise} - \Delta(3,4)_{noise} - \Delta(2,4)_{cw} + \Delta(3,4)_{cw}\right] + \\ &\quad \Delta(2,4)_{cw} - \Delta(3,4)_{cw} - \Delta(3,4)_{dynamic} \end{aligned} \tag{3}$$

where the number pairs indicate a calibration measurement from the first number to the second number, and the subscripts indicate the type of measurement made. The subscript cw indicates that a "continuous wave" source is used and "dynamic" indicates that this is the dynamic calibration of the receiver chain that is to be performed periodically perhaps even on a volume scan to volume scan basis. Following the NSSL EC method, the built-in calibration-maintenance function injects a variable-amplitude CW signal at point 3 and is measured at point 4 to obtain the differential tracking loss between receive channels

Waveguide Coupler Specifications	
Freq. Band	2.7–3.0 GHz
Coupling	44.2 ±0.3 dB
Coupling Variation	±0.2 dB
Coupling Calibration	±0.2 dB
Directivity	25 dBm
Insertion Loss	0.05 dB maximum
SWR Primary	1.05
SWR Secondary	1.10

Table 1: *Specification for WSR-88D waveguide coupler.*

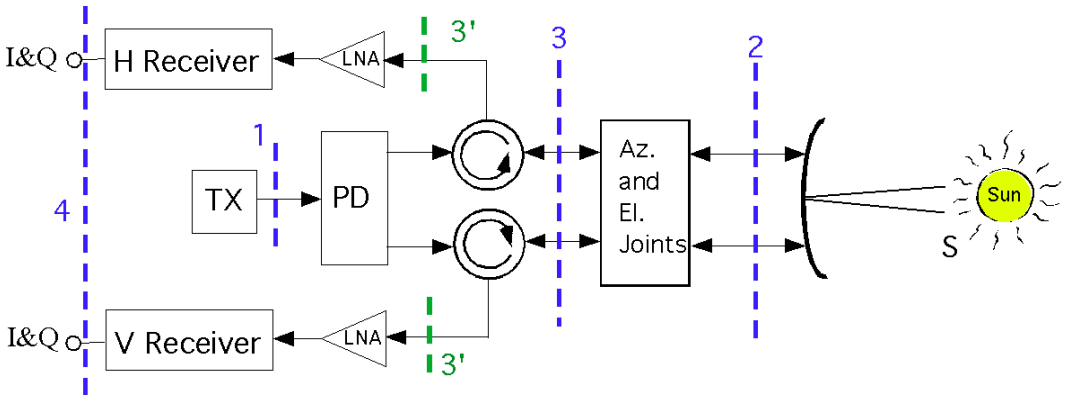

Figure 4: *An alternate block diagram of a radar system for the EC method. Compare to Fig. 3*

as a function of signal strength. The differential gain from point 3 to 4, containing the active circuits, will likely vary more than a minimum 0.1 dB and thus likely needs to be evaluated each volume scan. There is to be numerical compensation for active path differential nonlinearity measured from point 3 to 4. One-time fixed bias removal suffices for the passive paths.

Using these measurements, at least in principle, the differential gain of the entire radar system is known and Z_{dr} can be calibrated. However, in practice it is difficult to determine the measurement error. For example, waveguide couplers represent a crucial component in the absolute measurement of radio frequency (RF) power. Consider the current WSR-88D elevation arm coupler which is specified in Table 1. Though the impedance match specification (SWR) appears within acceptable limits for this application, the coupling factor accuracy specification (±0.3 dB) is larger than the desired 0.1 dB Z_{dr} uncertainty. The evaluation of the uncertainty of RF power measurements using such waveguide couplers is of central importance to the EC technique and is addressed later.

3.2 *Other Engineering Calibration Techniques*

Since the beginning of this Z_{dr} calibration evaluation project, other possible EC methods have come to light and in this report four EC methods are analyzed: 1) the original NSSL "long" EC method also referred to as the two coupler method, 2) the new NSSL "short" method, 3) the NCAR one coupler method and 4) the S-Pol legacy technique. To explain the differences between among these four methods, consider the radar block diagram given in Fig. 4 which is equivalent to Fig. 3. The measurements "planes" are shown by the blue (and one green) dashed lines. "PD" stands for power division, and "TX" stands

for transmitter. The S represent the sun's radiation. The numbers refer to the identical locations as in Fig. 3. For the KOUN radar, the green dashed line shows the location measurement plane 3 while the blue number 3 measurement plane is used by S-Pol. This difference is noted, however, it does not affect the results of our Z_{dr} calibration analysis (unless the circulators are significantly temperature dependent). The NSSL long method is referred to as the two coupler method since RF power measurements are made with respect to two reference planes, namely, "2" and "3".

In the NSSL short method, the transmit path is characterized by just one measurement: the measurement of differential transmit power at reference plane "2". The differential gain of the path from reference plane "2" to outside the radome is considered negligible and is ignored. The transmit path is characterized by passive solar measurement, i.e., from the sun to the I&Q sample. Thus, the NSSL short Z_{dr} calibration equation becomes,

$$Z_{dr}^{bias} = \Delta(1,2)_{pulse} + \Delta(S,4)_{noise}. \tag{4}$$

The dynamic calibration of Z_{dr} is achieved as follows: immediately after performing the EC calibration, a dynamic differential calibration of the active portion of the receiver path is performed (i.e., from plane 3 to plane 4). Since the radar is calibrated, this dynamic calibration is considered a base line. If subsequent dynamic calibrations differ from the base line measurement, the offset between the the two is considered to be a Z_{dr} bias caused by drifts in the active receiver path (e.g., due to changes in temperature). Measured Z_{dr} then is adjusted by this offset value.

The NCAR EC method is similar to the short NSSL method but with the addition of one more measurement: the differential power measurement from plane "2" to plane "4". In this way, the complete transmit and receiver paths are accounted for. The calibration equation becomes,

$$Z_{dr}^{bias} = \Delta(1,2)_{pulse} + 2\Delta(S,4)_{noise} - \Delta(2,4)_{noise}. \tag{5}$$

This is referred to as the one coupler method since the two RF power measurements are made with reference to just one plane, namely, plane 2[1]. As is show later, the Z_{dr} uncertainty is smallest for this EC method since the H and V couplers are used to both inject signal as well as measure signal (compare to the NSSL short method) and there is a minimum of couplers used (compare to NSSL long method). When the same couplers are used to both measure power as well as inject power in the calibration process, some of the uncertainty due to the waveguide couplers cancel.

3.3 *RF Power Measurements*

Consider the problem of measuring the power flowing inside a waveguide. To do so requires

1. Waveguide coupler
2. Calibrated bolometer power sensor
3. Precision attenuator, adapters and cables
4. Calibrated power meter instrument
5. Procedures and recording

[1]Plane 3 could be used equally as well as plane 2, i.e., Eq. (5) becomes $Z_{dr}^{bias} = \Delta(1,3)_{pulse} + 2\Delta(S,4)_{noise} - \Delta(3,4)_{noise}$

At each hardware connector junction there will be an impedance mismatch that will give rise to unknown reflections (unless this is measured with a high quality network analyzer). Additional uncertainties are associated with the coupler, the bolometer and the power meter instrument. Uncertainty budget analysis for the components used with S-Pol indicates that waveguide absolute power measurements in the field (for example with the HP436A instrument and HP8481A sensor) have a combined uncertainty of about 0.20 dB and the uncertainty of ratio (differential) measurements of about 0.18 dB. If instrumentation corrections are made, these 2σ uncertainty numbers may be reduced to about 0.12 dB and 0.05 dB respectively. To achieve this, the waveguide coupler must be of high quality and have side arm coupling factor of approximately 40 dB and high directivity better than 30 dB. The *forward port coupling factor must be known and maintained to 0.05 dB,* and the equivalent mismatch of the side arm port and of the power meter must be known and maintained to within 0.02 dB. These will be difficult standards to not only attain by maintain.

In addition to these specifications, the *calibration procedure* will also contribute to the uncertainty. Different technicians use measurement equipment differently. Repeatedly connecting and disconnecting equipment can and will change impedance mismatches. Thus, the use of automated test equipment (ATE) will minimize these sources of errors and uncertainty and the ATE designed and developed at NCAR is discussed next.

3.4 *Automated Test Equipment System (ATE)*

Mechanical processes and procedures such as attaching and re-attaching cables, couplers and meters introduce variability to the EC approach. To reduce these effects, Automatic Test Equipment (ATE) has now been built into S-Pol to measure test point signals, inject test signals and monitor environmental variables such as temperature along the signal path using fixed cable attachments and electronic switches. Figure 5 shows a block diagram of S-Pol. The green box shows the ATE with its multiple input and output lines marked in yellow. The shown yellow connectors (small circles) are connected to the other Test Points also marked in yellow. The S-Pol system has two parallel processors: 1) the VIRAQ (developed by NCAR) and 2) the SIGMET RVP8.

The transmit RF signal (red box) goes through a power distribution network which provides for 1) fast alternating H and V polarization transmission (pulse to pulse) via a mechanical switch 2) simultaneous H and V transmission via a power divider, 3) H only transmission and 4) V only transmission. The transmit signal(s) pass through the circulators, Test Point 3, rotary joints, Test Point 2 and then to the antenna/dish. The received signal passes back through to the circulators and then through the LNAs (low noise amplifiers). Physically, the transmitter, the circulators, the LNAs and the remaining receiver and processor circuits are all located in the S-Pol "transmitter trailer". After demodulation to IF (intermediate frequency), the signals pass through a switch shown in blue. The switch can direct the IF signals to either IF amplifier #1 (called copolar amp.) or IF amplifier #2 (called crosspolar amp.). When operating in fast alternating H and V transmission mode, the switch is typically used to direct the copolar signals to the same IF amplifier so that any temporal variation in the IF amplifier and remaining sections of the receiver/processor will affect both copolar signals equally. This is done to reduce the variance of Z_{dr} measurements. Thus S-Pol has four separate receiver paths to calibrate: 1) H signal to IF amp #1, 2) H signal to IF amp #2, 3) V signal to IF amp #1, and 4) V signal to IF amp #2. Test Point 4 yields the digitized in phase and quadrature (I and Q) samples (see http://www.eol.ucar.edu/rsf/spol/spol.html for a description of S-Pol).

Inside the ATE is a control computer, wideband power meter, signal generator, noise sources, attenuators and an RF switching matrix, all of quality necessary to achieve overall 0.1 dB measurement

uncertainty. Appropriate control connections are established between the ATE and the digital receiver, transmitter, and antenna pedestal. The ATE records the process measurements and the radar scans of the sun. Over a period of months a data base will be created so that a statistical analysis of the calibration measurements will ultimately lead to an estimate of the uncertainty of the EC Z_{dr} method (and aid in the evaluation of the other techniques also). Data from the VP approach will be used with ATE data to evaluate the EC approach. An EC method is routinely employed at both CSU-CHILL and S-Pol, however, it typically has been found that a systematic Z_{dr} bias persists which must be corrected using vertical pointing data in light rain.

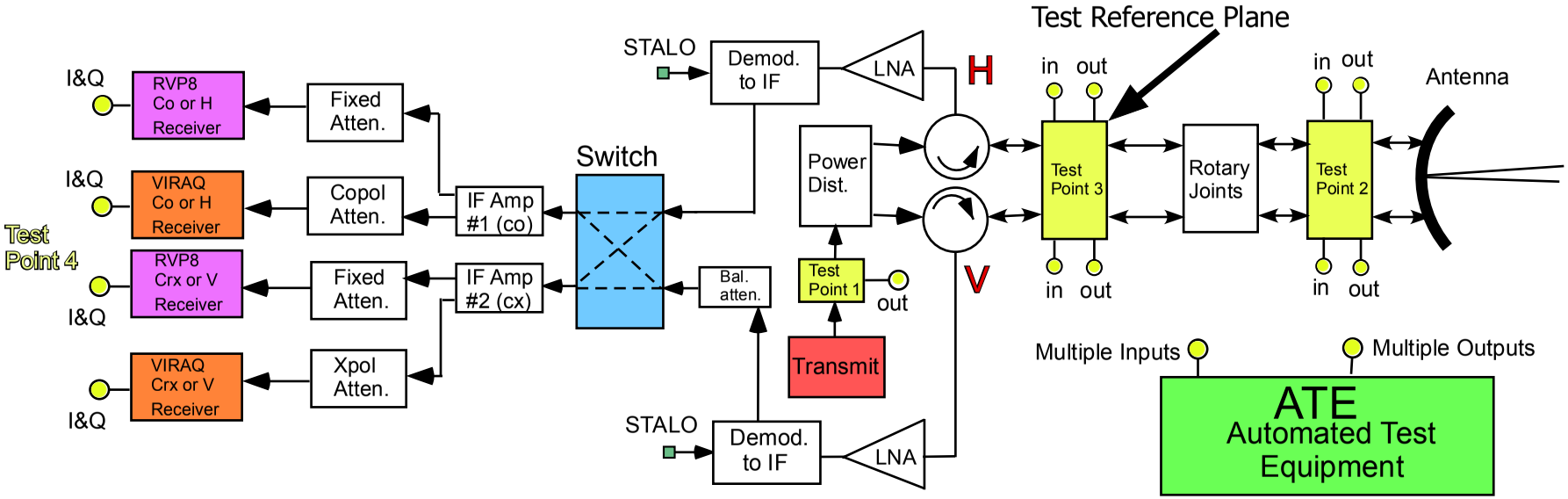

Figure 5: *A block diagram of S-Pol showing the Automated Test Equipment and Test Points that correspond to Fig. 3*

.

Uncertainty	Description	value (dB)
U_s	Waveguide coupling factor	0.10
U_s	Switch jitter	0.04
U_a	Attenuator	0.08
U_p	Power sensor (RF to DC)	0.09
U_m	Power meter	0.05
$U_{w,c}$	Impedance mismatch between waveguide coupler and waveguide	0.06
$U_{c,s}$	Impedance mismatch between waveguide coupler and switch	0.06
$U_{s,a}$	Impedance mismatch between switch and attenuator	0.06
$U_{a,p}$	Impedance mismatch between attenuator and power sensor	0.02
$U_{g,s}$	Impedance mismatch between generator and switch	0.06
U_{gn}	generator noise	0.02
U_{gn}	Sun source & processing	0.05

Table 2: *A list of 2σuncertainties for the differential power measurement shown in Fig. 7 .*

3.5 *The uncertainty of the EC method*

In this section some of the uncertainties of making a power measurement from a waveguide are given and the uncertainties are then applied to a differential waveguide power measurements. Finally, these measurements are applied to the estimation of the uncertainty of the NCAR EC short method. Shown in Fig. 6 is a picture of an experimental power measurement from inside the transmitter trailer at S-Pol. The H and V waveguide are seen at the top of the picture. The waveguide couplers are blue and connected to waveguide coupler can be seen the attenuator, power sensor and power meter. For this setup, the attenuator would be disconnected from one waveguide coupler and attached to the other waveguide coupler to complete the differential power measurements. Figure 7 shows a block diagram for a differential power measurement. In this setup (modeled after the ATE) a switch is used to select either the H or V waveguide for measurement. Shown also are circles that indicate some of the various uncertainties that affect the power measurement. Table 2 gives a description of the uncertainties and typical values (2σ coverage, for high quality, well calibrated test equipment).

The uncertainty of H and V measured power can be expressed

$$U_m^H = f\left(U_c^H, U_{w,c}^H, U_{w,s}^H, U_s, U_{s,a}, U_a, U_{a,p}, U_p, U_m\right) \quad (6)$$

$$U_m^V = f\left(U_c^V, U_{w,c}^V, U_{w,s}^V, U_s, U_{s,a}, U_a, U_{a,p}, U_p, U_m\right) \quad (7)$$

where the superscripts indicate the H or V channel and the subscripts indicate the source of the uncertainty. These uncertainties, which are in dB and therefore are fractional uncertainties, are assumed independent and thus are combined in quadrature (see Appendix A). Using the uncertainties listed in Table 2, $U_m^H = U_m^V = 0.19\,dB$. The uncertainties in Table 2 are either manufacturer specifications or are uncertainties due to impedance mismatch. The impedance mismatch uncertainties are are discussed below. As can be seen from Eqs. (6) and (7), there are several common uncertainty sources for the H and V power measurements so that the uncertainty of the differential waveguide power measurement becomes,

$$U_m^D = f\left(U_c^H, U_{w,c}^H, U_{w,s}^H, U_c^V, U_{w,c}^V, U_{w,s}^V\right) \quad (8)$$

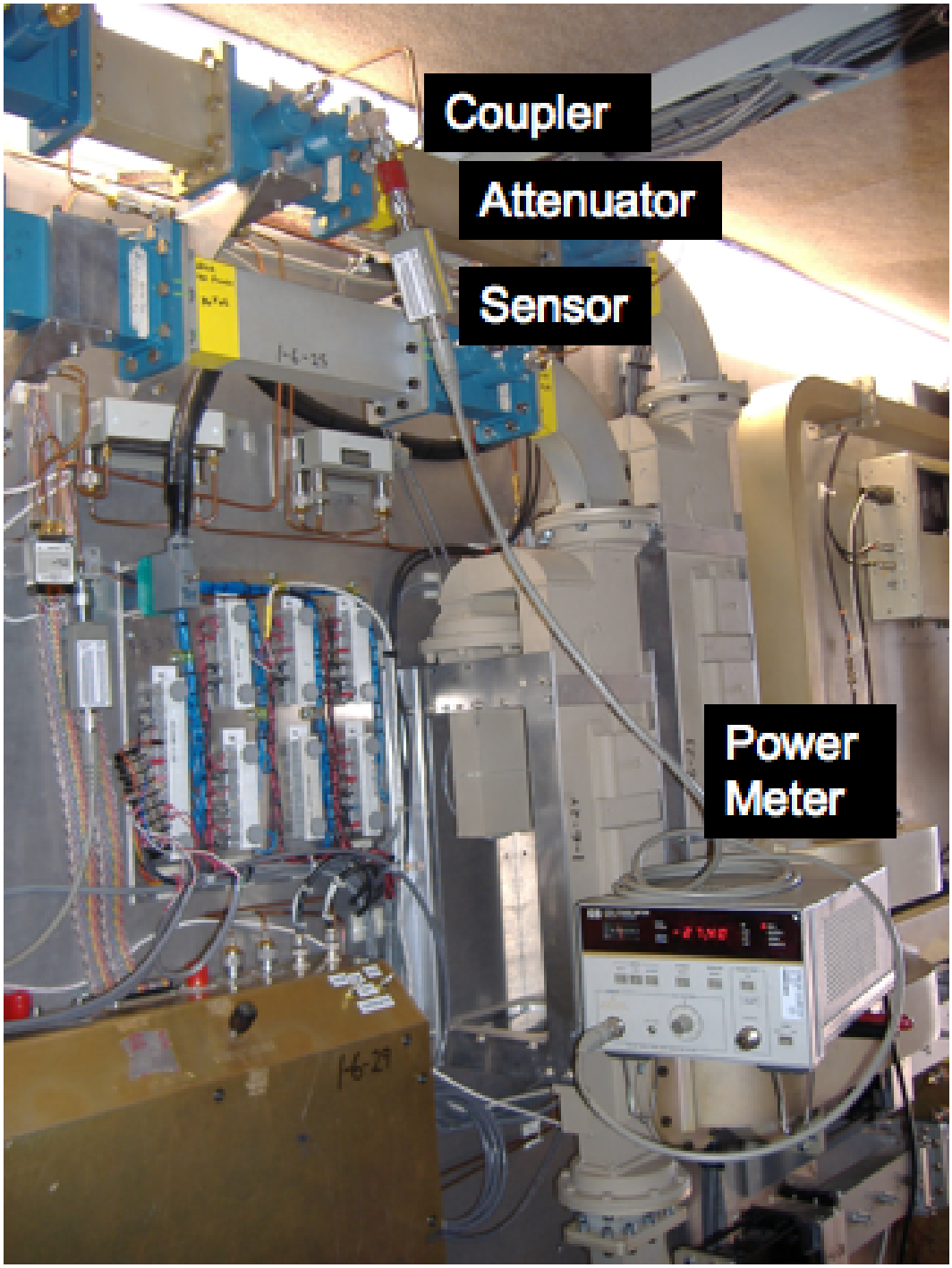

Figure 6: *A picture of a power measurement made inside the S-Pol transmitter trailer.*

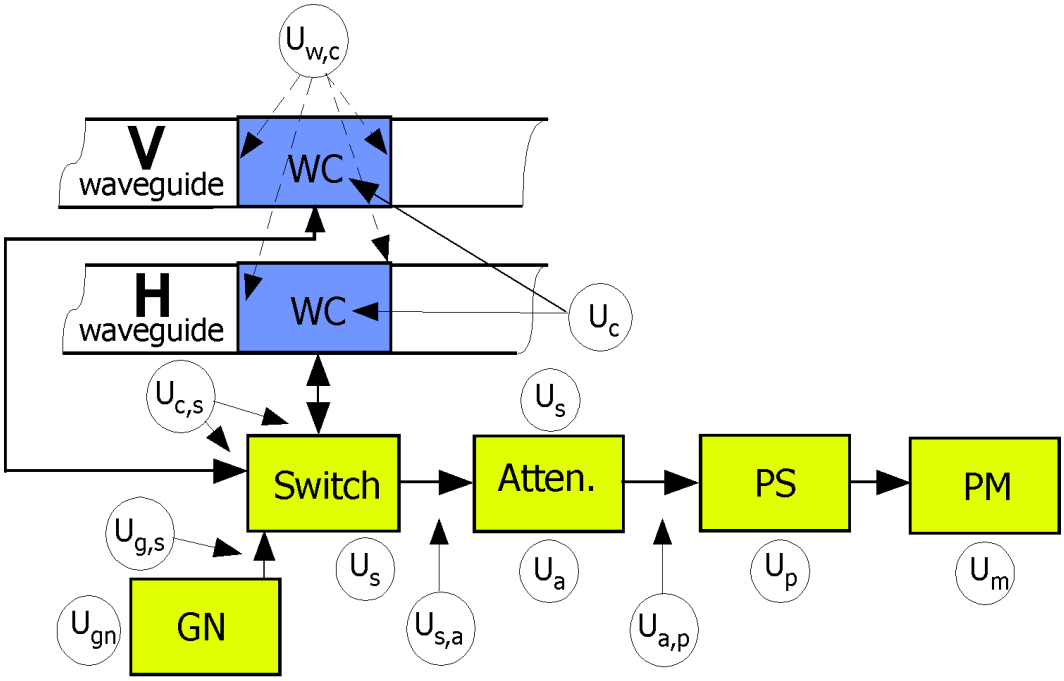

Figure 7: *A block diagram of a differential waveguide power measurement. "WC" is waveguide coupler, "Atten." is an attenuator, "PS" is a power sensor, "PM" is a power meter and "GN" is a generator. The circles represent the various uncertainties. The double subscripted uncertainties are various impedance mismatches between the devices. A list of the uncertainties with definitions is given in Table 2.*

where U_m^D is the differential power measurement uncertainty. Even though the uncertainty due to the instrumentation cancels, there are the additional uncertainties due to the extra waveguide coupler (0.1 dB) and the associated impedance mismatches. Again, the uncertainties are assumed independent and are combined in quadrature to yield an expanded uncertainty of 0.18 dB.

This uncertainty can be regarded as the uncertainty of the $\Delta(1,2)$ term in the EC calibration Eqs. (3), (4) and (5) where the transmit pulse power is measured at test plane 2. If the same waveguide couplers are used to inject signals for the purposed of determining the $\Delta(2,4)$, more of these uncertainty terms in Eq. (8) will cancel when calculating the overall uncertainty of Eq. (5). Specifically, the uncertainty of the waveguide coupling factor, U_c, will cancel. *However,*

An important observation is that the coupling factor for a waveguide coupler is bi-directional or reciprocal where as the impedance mismatch factors are not reciprocal.

Thus, if a signal is injected via the switch in Fig. 7 for the purpose of measuring $\Delta(2,4)$, when calculating the uncertainty of Eq. (5), the waveguide coupler uncertainty factor will cancel. However, the uncertainties due to impedance mismatch will not cancel due to the non reciprocity of these factors (this can be attributed to the different load impedances seen). The total uncertainty of Eq. (5) can be expressed

$$U_m^T = f\left(U_{w,c}^{H_{inj}}, U_{w,s}^{H_{inj}}, U_{w,c}^{V_{inj}}, U_{w,s}^{V_{inj}}, U_{w,c}^{H_{out}} U_{w,s}^{H_{out}}, U_{w,c}^{V_{out}}, U_{w,s}^{V_{out}}, U_s, U_{gn}, U_{g,s}, U_{sun}, U_{tx}, U_D\right) \tag{9}$$

where the "inj" denotes the impedance mismatch at the waveguide coupler interfaces when signal is being injected into the waveguide, the "out" denotes the impedance mismatch at the waveguide coupler interfaces when signal is being sampled from the waveguide. As can be seen from Eq. (9), the uncertainty of making a Z_{dr} bias estimate via Eq. (5) is due in large part to impedance mismatches. Other uncertainties are U_{gn} the signal generator noise, U_s switch jitter and U_{sun} sun variability and processing procedures (0.05 dB), U_D dynamic measurement errors and drifts (0.05 dB), and U_{tx} the power injection uncertainty for the measurement $\Delta(1,2)$ (0.05dB). The impedance mismatches are quite significant and the 2σ uncertainty estimate due to just just the 8 waveguide impedance mismatch terms is 0.17 dB (i.e., adding the 8 individual uncertainty estimate of 0.06 dB in quadrature). Adding the rest of the uncertainties yields $U_m^T = 0.2\,dB$. The uncertainties used are taken from Table 2 where we assume $U_{w,c}^{H_{inj}} = U_{w,c}^{H_{out}} = U_{w,c}^{H}$ and similarly for the other impedance mismatches.

a) Impedance mismatch factors For each component interface a connection of some sort needs to be made and for each connection there will exist an impedance mismatch that will give rise to unknown reflected signal that will alter the power measurement. Each mismatch alteration is itself deterministic and may be corrected if the relevant scattering parameters of the junction are known, however this correction is complex.

Though vector power measurements are deterministic, scalar power measurements cannot be considered such because of the unknown signal reflection coefficients at the connections. The error components for this evaluation tend to be small compared to the error limits of test equipment and procedures. This is termed a low "accuracy ratio". The uncertainty performance of the calibration measurement process must be better than the measurement uncertainty of the instrument being calibrated. That is the "accuracy ratio".

The reflection coefficient (Γ) is a complex number closely related to scattering parameters S_{11} and S_{22} of two-port junctions. Return loss in decibels and voltage standing wave ratio (VSWR), cited in component specifications, is related to the magnitude of reflection coefficient $|\Gamma|$ as follows

$$\begin{aligned} RL_{dB} &= 20\log(|\Gamma|) \\ VSWR &= (1+|\Gamma|)/(1-|\Gamma|) \\ |\Gamma| &= (1-VSWR)/(VSWR+1) \end{aligned} \tag{10}$$

For evaluation of mismatch we employ the following power transfer equations

$$P_{ds} = M_{gs} P_{ag} \tag{11}$$

$$P_{dl} = M_{gl} P_{ag} \tag{12}$$

where P_{ds} is the power delivered to the power sensor, P_{dl} is the power delivered to the load, if different from the sensor, M_{gs} and M_{gl} are the mismatch factors, and P_{ag} is the available power from the generator. M_{gs} and M_{gl} range between 0 and 1 depending on how well the match conditions for maximum power transfer are satisfied (Kearns and Beatty 1967).

$$M_{gs} = (1-|\Gamma_g|^2)(1-|\Gamma_s|^2)/(|1-\Gamma_g\Gamma_s|^2) \tag{13}$$

In Table 3, the magnitudes of typical impedance mismatch uncertainties from (13) are presented, corresponding to return losses of approximately -30 dB, -20 dB, and -15 dB typically found for microwave

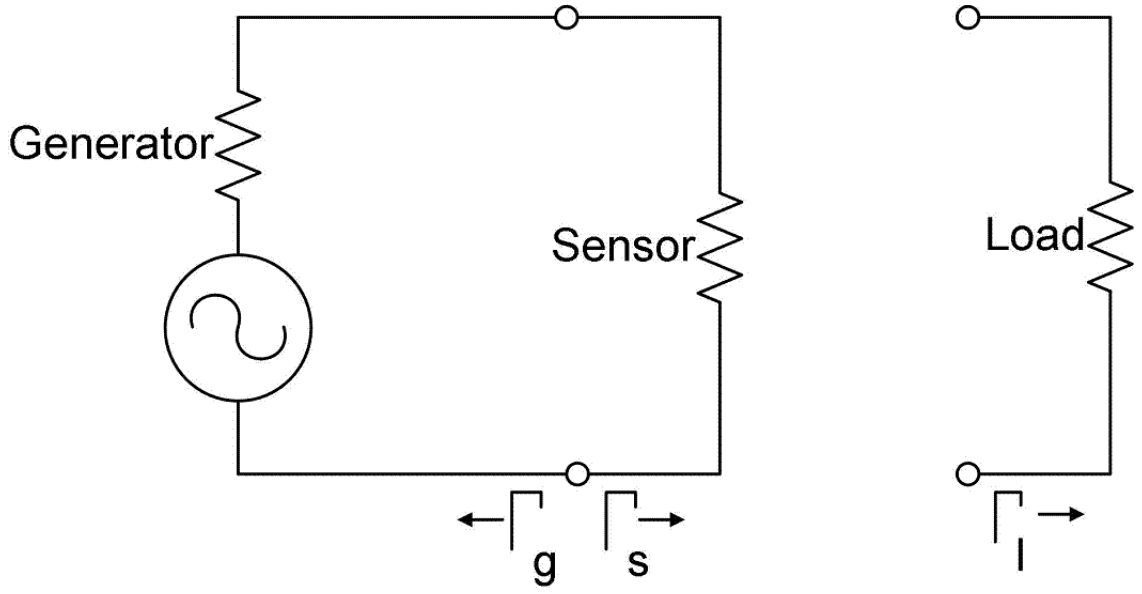

Figure 8: *Basic circuit for mismatch error evaluation of power delivered to a sensor and to a directly substituted load. A two-port microwave junction, such as an attenuator or a cable, may be placed between the generator and load.*

						Model A	**Model B**
						U$\|\Gamma_l\|$	**Const**$\|\Gamma_l\|$
$\|\Gamma_l\|$	VSWR	RL load	RL load (dB)	Mu- (dB)	Mu+ (dB)	u(Mu) (dB)	u(Mu)
0.024	1.050	0.001	-32.256	-0.0052	0.0052	0.002	0.004
0.091	1.200	0.008	-20.828	-0.0721	0.0715	0.025	0.050
0.200	1.500	0.040	-13.979	-0.3546	0.3407	0.121	0.239

Table 3: *Relationship between reflection parameters and impedance mismatches selected to represent excellent, good, and average match conditions of a sensor connected to a generator having a return loss of -20 dB. See text for explanation of mismatch quantities shown in the four right-hand columns.*

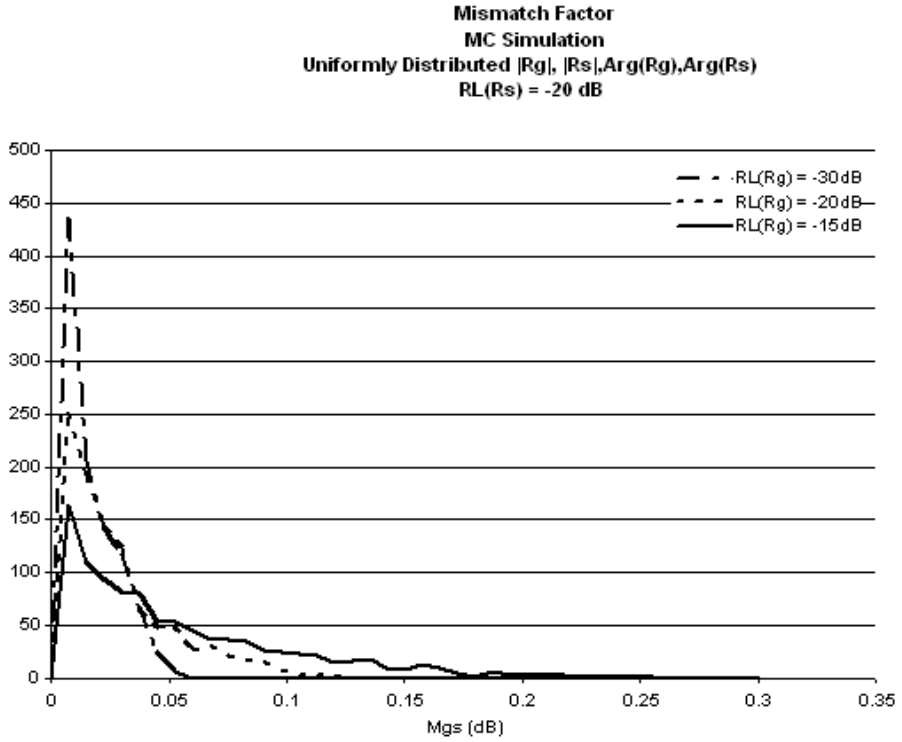

Figure 9: *Histogram of simulated (Monte Carlo, 1000 trials) mismatch factors based on a sensor return loss uniformly distributed up to -20 dB and generator return loss uniformly distributed up to -30 dB, -20 dB, and -15 dB, and uniformly distributed phases.*

radar system components. Table 3 shows the magnitude of mismatch errors that occur at a power measurement interface when a load with excellent, good, or fair match is connected to a generator with good match. It is evident that controlling the VSWR of each junction to a maximum of 1.2, but preferably better under various measurement conditions, is essential to reach the goal of 0.1dB expanded uncertainty. Mu+ and Mu- are the uncertainties at worst-case phase angles. The column labeled $U|\Gamma_l|$ is the calculated standard uncertainty under the assumption of a uniform distribution of reflection coefficient Γ_l and phase; the column Const$|\Gamma_l|$ assumes that the reflection coefficient Γ_l is as specified but again with uniform phase on each side of the interface (Agilent Technol. 2001).

The reader is reminded that though the right hand columns represent likely uncertainty at each measurement junction, there will be several such measurements that contribute to the combined uncertainty.

Mismatch errors do not possess normal distributions and have been further evaluated with Monte Carlo simulations. Results are shown in Figs. 9 and 10 corresponding to columns U$|\Gamma_l|$ and Const$|\Gamma_l|$ of Table 3. The distributions are not Gaussian and show the potential of fairly large errors even for well matched components. Either the impedance match of components must be carefully controlled for these scalar power measurements, or the more difficult vector power measurements may be used.

Most microwave measurement texts and articles devote a substantial percentage to treatment of ways to mitigate mismatch effects for precise power measurement. Many of the assumptions made regarding impedance mismatches are tantamount to assuming reciprocity: the implicit impedance matches are "stationary" and reciprocal to a degree that is better than measurable (say 0.01 dB). This is subverted in at

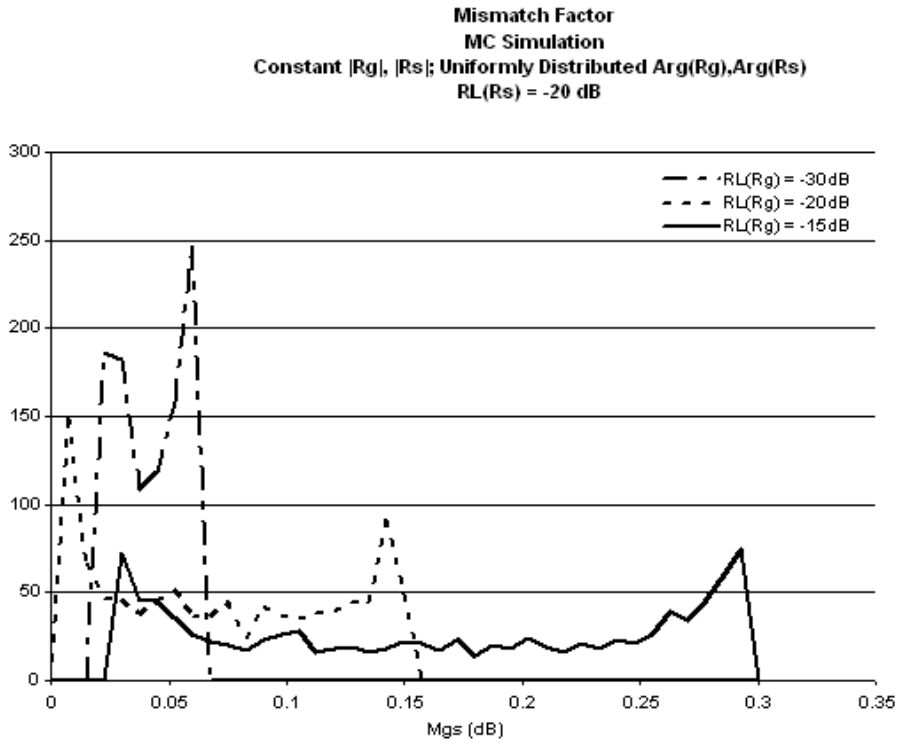

Figure 10: *Histogram of simulated (Monte Carlo, 1000 trials) mismatch factors based on a sensor return loss of a constant -20 dB and generator return loss constant at -30 dB, -20 dB, and -15 dB, and uniformly distributed phases.*

least two cases that we can think of: 1) a circulator will not have the same reflection coefficient when in transmit mode as when receiving and 2) the return loss of the antenna system will depend on antenna position by virtue of "wow" in the rotary joints and variable radome seam scattering. As an additional example, consider the measurement of the factor $\Delta(1,2)$ where a waveguide coupler is used at measurement plane 2. The load seen by the transmitter will be antenna system and this will govern the associated reflections and impedance mismatch will affect the power measurement. Next consider the evaluation of the factor $\Delta(2,4)$ which uses the same waveguide coupler but for signal injection this time. The load seen this time is governed primarily by the circulator and thus the impedance mismatch value and the associated reflections has changed even though the hardware connection have remained the same. This then is the bases of the 0.06 2σ uncertainty used for the impedance mismatches in Table 2.

4 CROSSPOLAR POWER APPROACH

The CP method has been successfully applied to the CSU-CHILL as well as S-Pol radar data to calibrate Z_{dr} (Hubbert et al. 2003; Hubbert et al. 2006). The technique uses the property of radar reciprocity (Saxon 1955) which states that the off diagonal terms of the radar scattering matrix, S_{hv}, S_{vh}, are equal (Bringi and Chandrasekar 2001). Using this fact the Z_{dr} calibration equation can be derived:

$$Z_{dr}^{cal} = Z_{dr}^{m} S^2 \frac{\overline{P_{xv}}}{\overline{P_{xh}}} \tag{14}$$

where Z_{dr}^{cal} is calibrated Z_{dr}, Z_{dr}^{m} is measured Z_{dr}, S is the ratio of the V and H power from sun measurements, and $\overline{P_{xh}}$, $\overline{P_{xv}}$ are the average transmit H and transmit V crosspolar powers, respectively. The crosspolar powers may be averaged over a few rays or an entire volume of radar data. Both precipitation as well as ground clutter targets may be used. If precipitation targets are used, fast alternating H and V transmit polarizations must be used. The CP Z_{dr} calibration approach is like the VP technique in that neither require waveguide couplers, signal sources nor power meters and thus the associated uncertainty related to such RF measurements is eliminated.

S-Pol employs a copolar and crosspolar receiver design in contrast to H and V receivers as described in Section 3.4. This is done to reduce the variance and drift of the Z_{dr} measurement but this also slightly changes the Z_{dr} calibration equation to:

$$Z_{dr}^{cal} = Z_{dr}^{m} S_1 S_2 \frac{\overline{P_{xv}}}{\overline{P_{xh}}} \tag{15}$$

where S_1 is the ratio of V-copolar to H-copolar sun radiation and S_2 is the ratio of V crosspolar to H crosspolar sun radiation (See Hubbert et al. 2003 for details).

5 Z_{dr} CALIBRATION ISSUES FOR NEXRAD

Since NEXRAD will use simultaneous H and V polarization transmission to achieve dual polarization (Doviak et al. 2000), the Z_{dr} calibration procedure will need to be modified for the CP method. With fast alternating H and V transmission, the H and V crosspolar powers can be obtained essentially simultaneously. This is not the case for simultaneous H and V transmission: the crosspolar powers are not available! However, for NEXRAD slow mechanical waveguide switches can be used that allow only H

polarization or only V polarization to be transmitted and thus both crosspolar powers could be measured. If indexed beams are used, the H and V crosspolar clutter powers from alternate transmit only H and only V scans should be equal and thus could be used to calculate the ratio $\overline{P_{xv}}/\overline{P_{xh}}$. Experimental S-Pol data is given in Section 6 that support this.

Additionally, NEXRAD by design will employ H and V receivers instead of copolar and crosspolar receivers. Since the H and V copolar powers, P_{co}^H, P_{co}^V, that yield $Z_{dr} = 10\log_{10}[P_{co}^H/P_{co}^V]$ are processed by separate receiver channels, there will likely be significant differential fluctuation of these measured powers over time periods of tens of minutes. Of particular concern are the NEXRAD LNAs which reside up in the pedestal where they are exposed to significant temperature swings. Thus, in order to maintain uncertainty of Z_{dr} calibration to 0.1 dB, the receiver chain differential gain will very likely need to be monitored. This may be accomplished by several means. One way is to repeatedly make sun scans. However, the sun is not be available at all times: during the night, shadowed by precipitation, or when located beyond the scanning capabilities of the radar. Another technique would be to again use the crosspolar power ratio measurements since

$$\frac{P_{xh}}{P_{xv}} = \frac{P_h^t G_v}{P_v^t G_h}. \tag{16}$$

where P_h^t and P_v^t are the H and V transmit powers and G_h and G_v are the H and V receiver gains. Thus, if the the transmit power ratio, P_h^t/P_v^t is constant over the measurement period, the ratio of crosspolar powers yields the differential gain of the receivers, G_v and G_h. This would require that the radar periodically make scans using transmit only H and only V. This obviously takes time and would cause wear on the mechanical switches. The third option, as mentioned above, is to inject test pulses into the receiver (before the low noise amplifiers), observe the I&Q output and in this way monitor any drift of the H and V receiver gains. The H and V gain curves of receiver chains are recorded when the initial calibration is accomplished. The difference of the two curves gives the Z_{dr} bias base-line. Any deviation from this base line curve found from subsequent test pulse measurements indicates a drift or bias in Z_{dr} and thus can be used to correct Z_{dr}.

6 EXPERIMENTAL RESULTS

In this section we present experimental results that are indicative of the uncertainty of the measurements that are required for the three Z_{dr} calibration techniques. Data come from both the RVP8 and VIRAQ processors. In the following analysis we assume that all systematic errors are negligible and thus we are estimating the uncertainty due to random errors. Any systematic error should be evident when the Z_{dr} biases calculated from the EC, CP and VP methods are compared.

6.1 *Sun measurement statistics*

The following data was gathered on 24 August 2006 using VIRAQ. Figure 11 shows a histogram of a set of 32-point, H-channel, sun-bore-sighted beam powers possessing a sample standard deviation of 1.04 dB. If 0.02 dB measurement uncertainty (see Appendix A) is desired, then about 13,800 integrated power measurements should be used to compute the mean power. This amount of data is easily obtained from sun scan measurements in about minute (depends on scan strategy).

The following data is processed by VIRAQ. On 8 August 2006, 13 consecutive "box scans" of the sun were made. The azimuth scan with the highest power point is selected and then the azimuth scan before

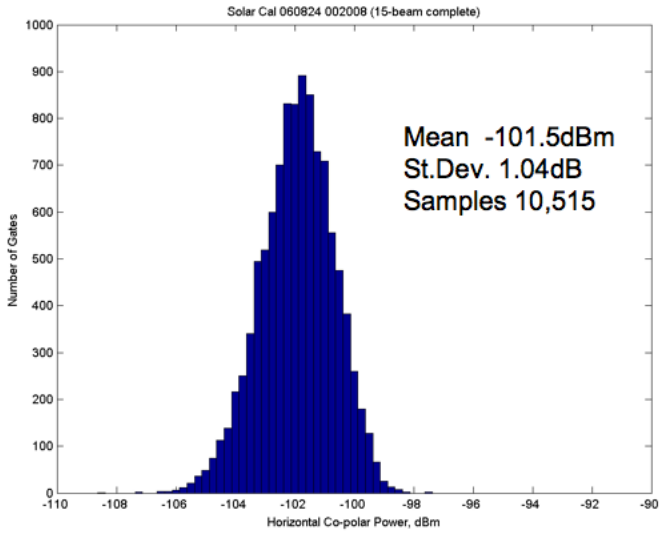

Figure 11: *Histogram of 32 point integrated sun power measurements.*

and after are also selected. Five beams are then selected from each scan centered on the beam with the highest power. Gates 150 through 950 are used and with 32 samples per gate and this gives a total number of I&Q samples of about 384,000. These samples are averaged for each box scan in order to estimate S_1 and S_2 that are required for the crosspolar power calibration technique. The calculated S_1S_2 numbers are (linear scale)

0.7760 0.7789 0.7854 0.7773 0.7843 0.7713 0.7795
0.7745 0.7812 0.7767 0.7744 0.7801 0.7732

The mean is 0.7780 with a standard deviation of 0.0042. The standard deviation is 0.023 dB and the 2σ uncertainty of the 0.7780 mean estimate is 0.0130 dB. This indicates that the uncertainty of the S_1S_2 product over a short time interval (about 0.5 hours) is well within the 0.1 dB uncertainty desired for NEXRAD Z_{dr} measurements.

a) Analysis of receive paths Recall that S_1 is defined as the ratio of V-copolar to H-copolar passive sun measurements (i.e., both V and H signals are processed by the copolar receiver). Referring to Fig. 5, the H-copolar signal path is from the antenna to the switch (blue box) through IF amplifier #1. [2] Likewise, the V-copolar path is from the antenna to the switch (blue box) through IF amplifier #1. Thus, the differential path of the H-copolar and V-copolar sun measurements is from the antenna to the input of IF amplifier #1 and the uncertainty of the above reported sun S_1 power ratio measurement is attributable to the differential gain variability of this path difference. Similarly, S_2 is defined as the ratio of H-crosspolar to V-crosspolar sun power measurements so that the differential path is from the antenna to the input of IF amplifier #2. Thus, the uncertainty of the S_1 and S_2 measurements should be very similar since the only signal path difference between the S_1 and S_2 measurements is through the switch, i.e., uncertainty in the measurement of both ratios quantify the differential gain variability of the H and V signal paths to the switch over the

[2]The path from IF amplifier #1 to the I&Q samples is defined as the copolar receiver and the path from IF amplifier #2 to the I&Q samples is defined as the crosspolar receiver

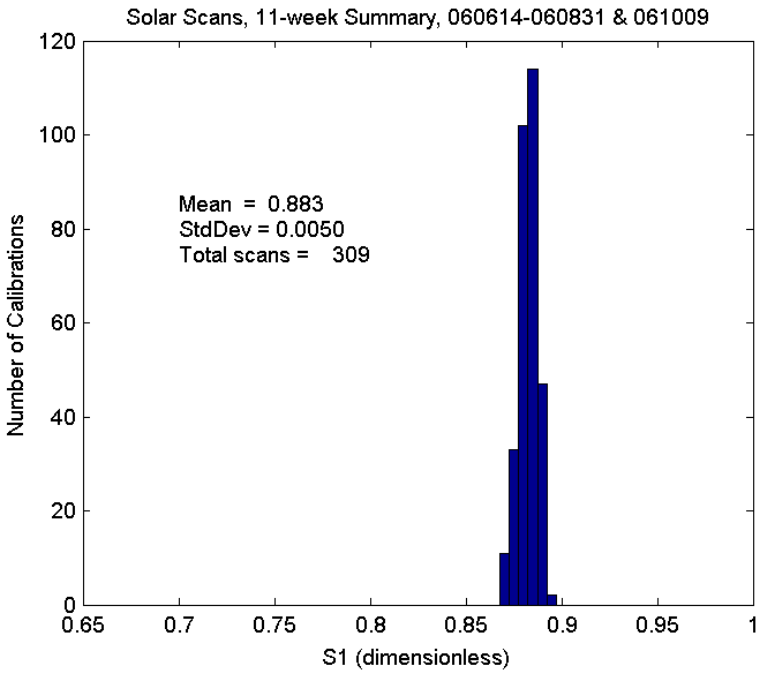

Figure 12: *Histogram of 309 S_1 ratio measurements.*

measurement period (neglecting the switch path differences).

Similarly, the differential path of H-copolar to H-crosspolar sun measurement ratio is from the IF amplifiers to the I and Q samples and thus measurements of this ratio quantify the differential gain variability due to the copolar to crosspolar receivers. Continuing, the differential path of H-copolar to V-crosspolar sun measurement ratio is over the entire sun signal path from the antenna to the I and Q samples. Thus, analysis of the various ratios of sun power measurements show the differential gain variance of 1) the copolar to crosspolar receivers (IF amps to I and Q samples), 2) the H and V receive paths (antenna to IF amplifiers) and 3) the entire receive path (from the antenna to the I and Q samples).

From 14 June to 24 August, 309 sun box scans were made and the mean ratios S_1 and S_2 were calculated. Figures 12 and 13 show histograms of these 309 values (linear scale). The means are 0.883 and 0.886, respectively, while the standard deviations are 0.005 and 0.006, respectively (all in linear scale). This yields a uncertainty (2σ) of 0.049 dB for S_1 and 0.058 for S_2 *over the entire 72 day measurement period*. Figure 14 shows the histogram of the product S_1S_2 and the mean is 0.781 with a standard deviation of 0.0091. The uncertainty is 0.10 dB. These Type A uncertainty values are likely dominated by variations in the gains of the LNAs since they are the only active component in the differential path. Figure 15 shows the time series of the S_1S_2 values. The plot indicates that although the variance of the S_1S_2 product is small, it should be monitored frequently in order to to keep the Z_{dr} calibration uncertainty under 0.1 dB.

Figure 16 shows the time series of 309 sun power measurements of H-copolar to H-crosspolar ratio. The plot shows an increasing trend from 0 to 40 on the scan number axis and there is also a spike at about 110 on the scan number axis. The exact cause of these anomalies is presently unknown but there were several system adjustments made during these time frames. The mean and standard deviation of the values from scan number 125 to 309 are 0.715 and 0.0041, respectively. The 2σ uncertainty is 0.050 dB. Again this uncertainty is due to gain fluctuations in the copolar and crosspolar receivers (IF amplifiers to

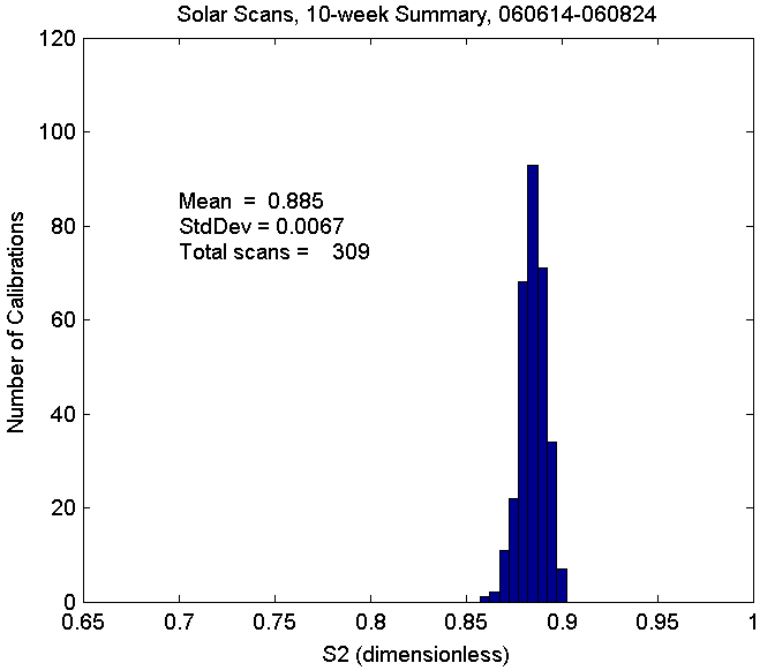

Figure 13: *Histogram of 309 S_2 ratio measurements (linear scale).*

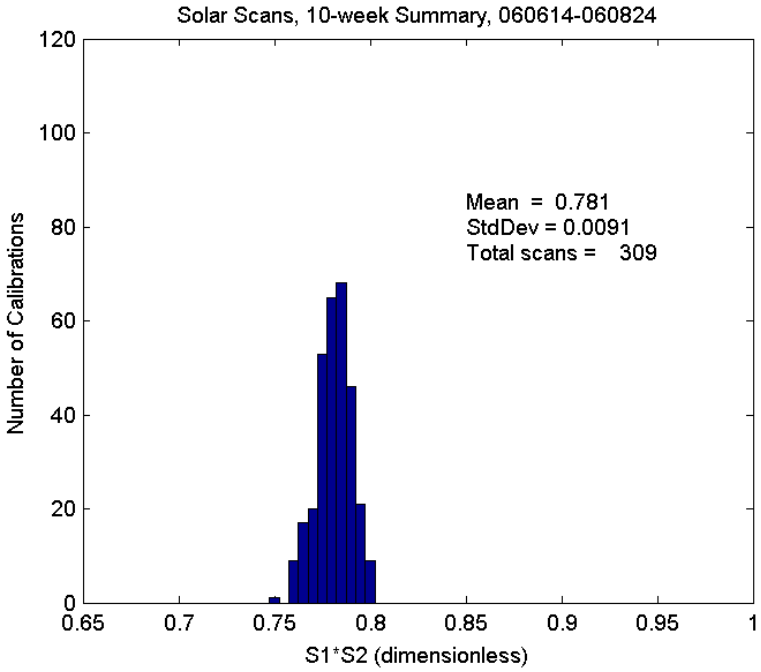

Figure 14: *Histogram of 309 S_1S_2 ratio measurements (linear scale).*

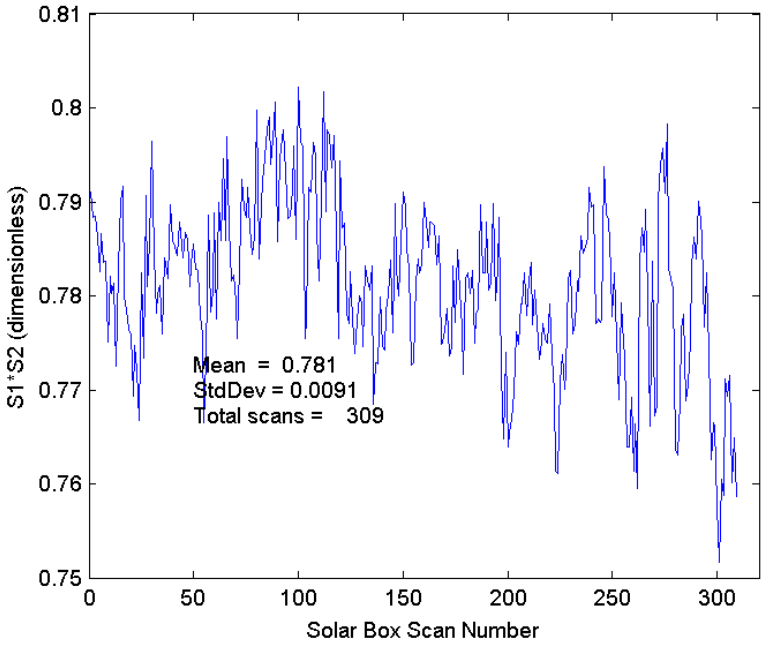

Figure 15: *Time series of the 309 S_1S_2 ratio measurements (linear scale).*

I and Q samples).

Figure 17 shows the time series of 309 sun power measurements of H-copolar to V-crosspolar ratio and the same anomalous features that are present in Fig. 16 are present here also. The mean and standard deviation of the values from scan number 125 to 309 are 0.811 and 0.0072, respectively. The 2σ uncertainty is 0.077 dB and this number is a measure of the differential gain variability of the entire differential receive path, i.e., from the antenna to the I and Q samples. If the uncertainty of H-copolar to V-copolar ratio (about 0.05 dB, see Fig. 14) is combined with the uncertainty of H-copolar to H-crosspolar ratio (.05 dB) via the root mean square rule (or quadrature rule) the result is 0.071 dB. This indirect estimate of the total differential gain uncertainty agrees very well with the direct estimate from the H-copolar to V-crosspolar measurements of 0.076 dB.

b) Type B sun calibration uncertainties: integration techniques and antenna patterns The above is a Type A evaluation of the uncertainty of sun power ratio measurements; Type B systematic errors could be present. Important in the above assessment of uncertainty is the integration technique used. Typically the sun is scanned with one tenth degree elevation steps at about one degree per second rate. Obviously, the precise location of the PPI elevation angle cuts through the sun will vary from one sun scan to another and this could affect the calculation of of the S_1S_2 ratio needed for Z_{dr} calibration. This is demonstrated in Fig. 18 which shows 301 sun calibration numbers (S_1S_2) gathered from June to September, 2006, for three different integration techniques. The three thin lines show the raw sun numbers while the thick lines are smoothed versions of the data.

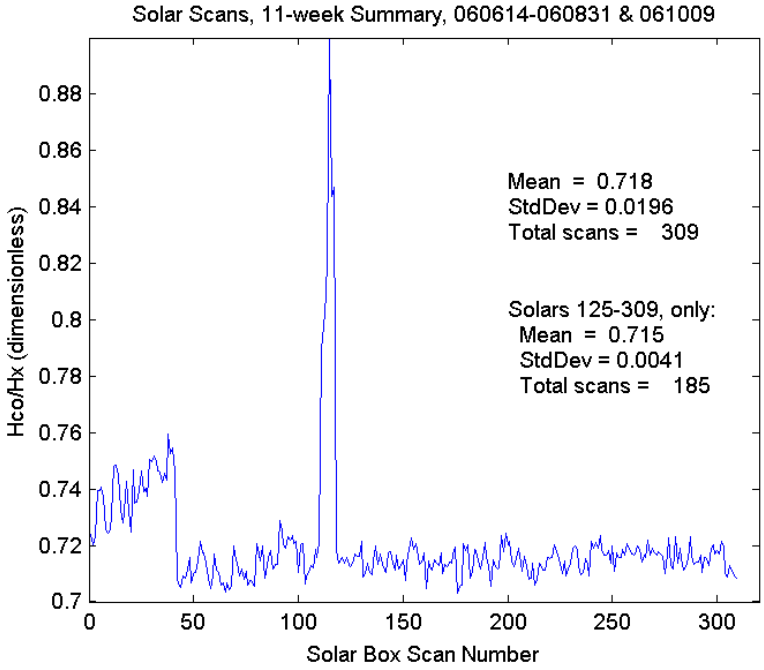

Figure 16: *Time series of 309 H-copolar to H-crosspolar sun power ratio measurements (linear scale).*

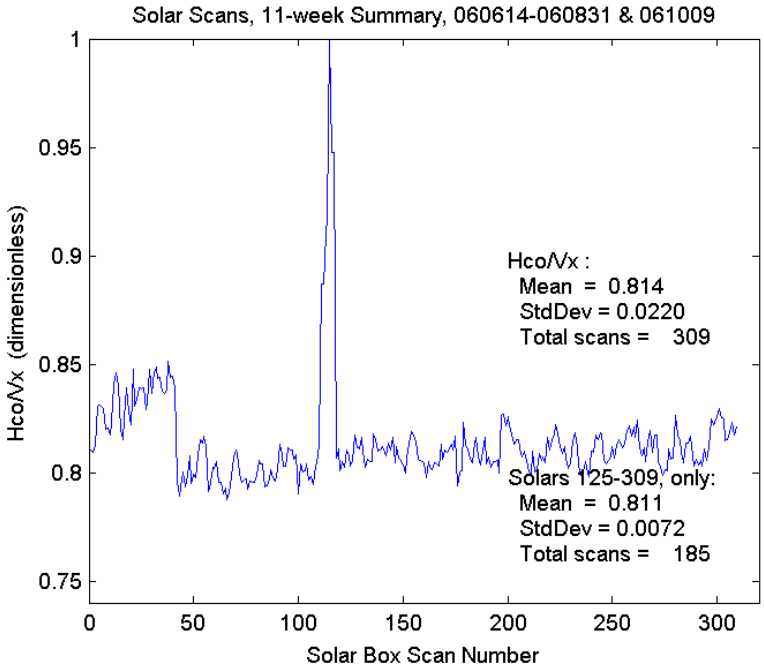

Figure 17: *Time series of the 309 H-copolar to V-crosspolar ratio measurements (linear scale).*

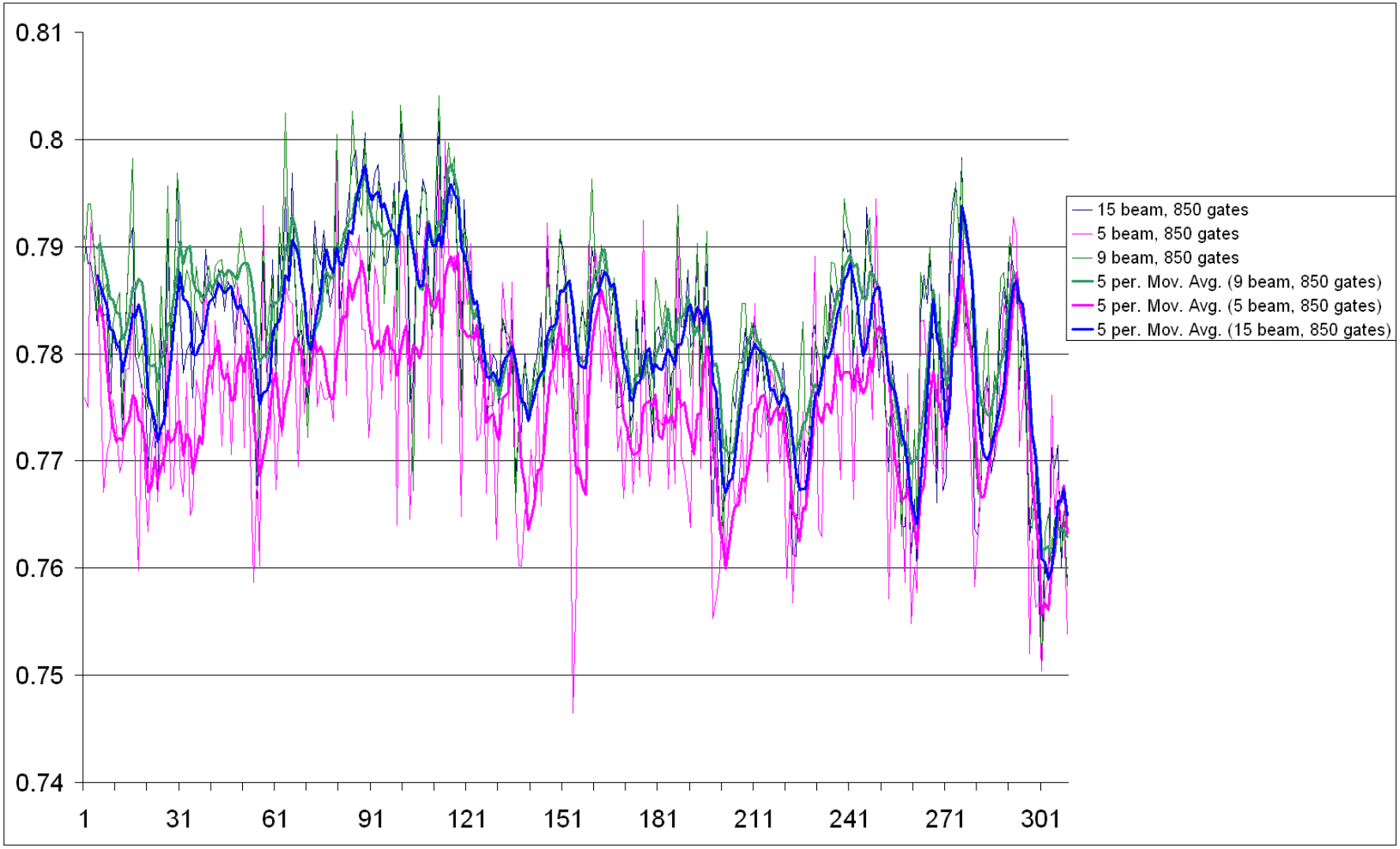

Figure 18: *Time series of S_1S_2 sun calibration measurements from July to September 2006. Data points are not equally spaced in time.*

Annuli	0.25°	0.50°	0.75°	1.00°	1.25°	1.50°	1.75°	2.00°
Mean (lin)	0.7762	0.7756	0.7755	0.7754	0.7754	0.7752	0.7752	0.7753
FSTD (dB)	0.0313	0.0261	0.0217	0.0214	0.0197	0.0212	0.0229	0.0277

Table 4: *The mean (linear) and the fractional standard deviation (FSTD)(dB) of sun scan data gathered from 26 July 2006 to 20 March 2007 for various annuli of integration centered on the sun maximum power.*

As described in Section 6.1, the PPI cut with the highest power is identified and then the PPI cuts just above and below the highest power cut are all selected for integration. The data is divided into 32 point range bins and three to five rays or beams of data are chosen for each PPI scan centered on the highest power beam. The three separate integrations are: 1) 3 PPIs with 5 beams each = 15 beams total (blue) 2) 1 PPI with 5 beams = 5 beams total (magenta) and 3) 3 PPIs with 3 beams = 9 beams total (green). These curves indeed show that the integration technique significantly affect the magnitude of S_1S_2. For example, consider the blue and magenta smoothed lines. The difference between them can be 0.015 or more in some areas and calculating the dB difference gives: $10\log_{10}(0.795/0.78) = 0.083$ dB, or nearly a tenth of a dB. Thus, a more consistent technique of processing the sun data is needed.

The following data is processed by RVP8. To reduce the sun integration errors, sun data points are first interpolated to a uniform rectangular $0.1^\circ \times 0.1^\circ$ grid. In order to determine the location of the sun center (considered the maximum power point), data along each of the vertical and horizontal grid lines are fitted to a Gaussian shaped curve and the location of the horizontal and vertical maximums of the Gaussian shaped curves are considered as the center of the sun. Note that the sun's center may not fall on on one of the grid points. The data is then integrated over different annuli corresponding to different radii. Fig. 19 shows the ratio S_1S_2 for sun scan data gathered from 26 July 2006 to 10 October 2007. The annuli of integration have 0.25° and 1.25° diameters. As can be seen the curves agree fairly well with the variance of the 0.25° curve (magenta) being greater than the variance of the 1.25° curve (yellow). The blue line corresponds to the integration technique in Fig. 18.

To further examine the effect of integrating the sun scans over various annuli, consider Table 4. Given in Table 4 are the means (liner units) and the fractional standard deviations (FSTD) (dB) calculated from 303 sun scans. The interpolation scheme combined either two or three sun scans to obtain one interpolated data set. There are 18 interpolated data sets that used two sun scans and 89 data sets that used three sun scans for a total of 107 interpolated sun scan data sets. Table 4 shows that the means of the sun scan data sets are nearly independent of the annulus of integration. The FSTDs are also similar but the lowest value is achieved for an annulus of 1.25°.

Such grided solar scan data can be used to construct "pseudo" antenna patterns. After compensating for the sun's movement and correcting for the radar elevation angle, the data can be used to construct "pseudo" antenna patterns in the sense that the distributed solar source is used instead of a point source. To estimate the true antenna pattern one would need to deconvolve the sun illumination pattern. The sun could be approximated as having uniform brightness over a disk that subtends about 0.53° though the sun behavior is considerably more complex. For a more full assessment of the sun's radiation see Tapping (2001), Kraus (1986) and Jursa (1985). Figures 20, 21 and 22 show the H, V and the H to V ratio antenna patterns. The H and V "pseudo" patterns are well matched across their 1° beam width but there is some difference outside these limits. To obtain non-biased Z_{dr} measurements of precipitation, the H and V antenna patterns must be well matched across their main lobes (Hubbert et al., Appendix C, 1998). Figure 23 shows the correlation between the measured H and V antenna patterns. Since the sun's

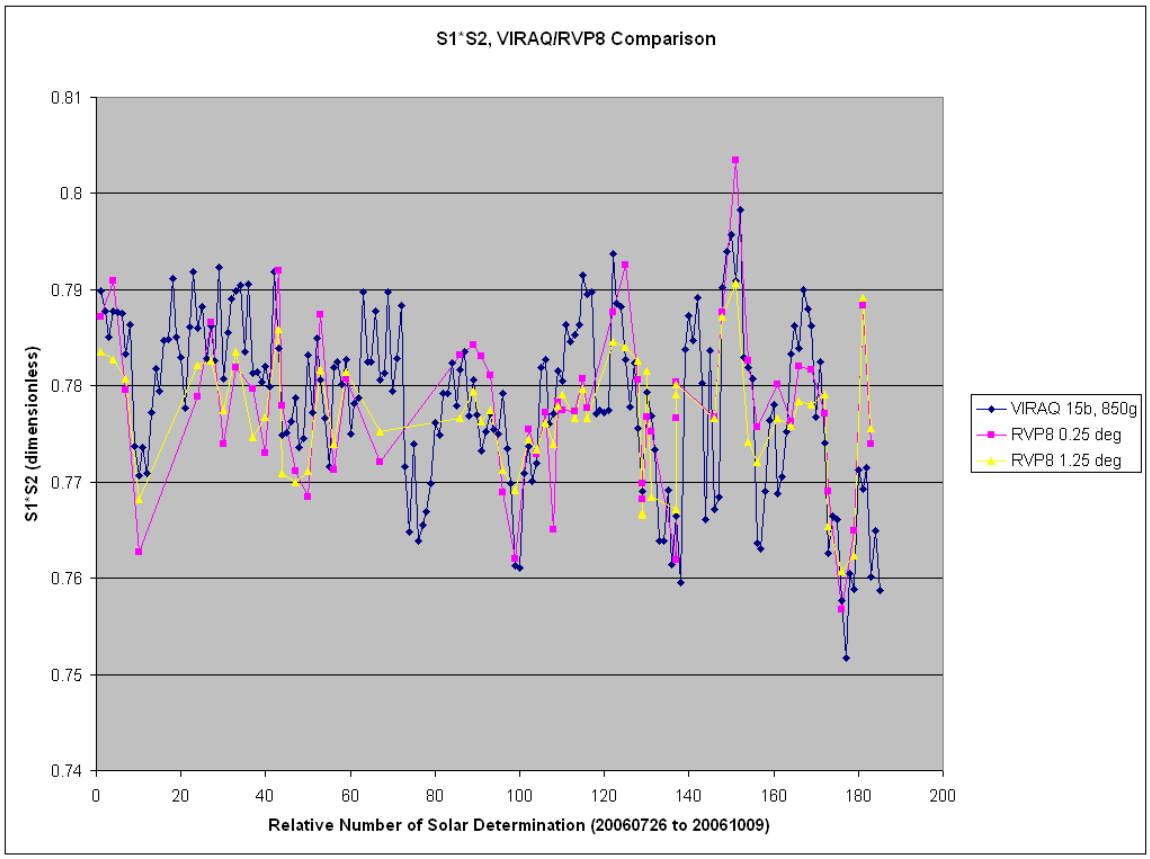

Figure 19: *Time series of mean values of S_1S_2 calculated from from sun scan data gathered from July 2006 through October 2006.*

radiation is unpolarized (there can be exceptions to this during high solar activity when the radiation can be circularly polarized) the expected correlation between the two patterns is 0. Figure 23 shows that the correlation over the center of the H and V antenna patterns is very low but there are four lobes of higher correlation. These four lobes are caused by the depolarization of the electric field by the four antenna reflector support struts.

To explain some of variance seen in S_1S_2 seen in Fig. 18, consider the differential antenna pattern of Fig 22. It is seen that more positive H/V values exist along the horizontal cut through the center whereas more negative values (in dB) exist along the vertical cut through the center. Thus, as more data is included from the center-top and center-bottom portions of the antenna pattern, more negative H/V ratios are expected. Since S_1S_2 is defined as V/H ratios, the blue line would be expected to lie above the magenta line as is shown in Fig. 18. Again, that integration technique simply used sun scan data along the PPI cuts of the sun. The more sophisticated sun data integration procedure first grids the data taking into account the sun's movement and the radar elevation angle and thus the region over which the sun scan data is integrated is much better controlled. Therefore, better sun statistics (less variance) are produced and the presence of possible systematic errors is reduced.

To gain further insight on the S_1S_2 ratio, the S_1S_2 ratio "antenna pattern" can also be calculated and is shown in Fig. 24. As can be seen the S_1S_2 pattern is fairly symmetric so that when integrating over the various annuli, the mean value does not change much. Finally, we compare the standard deviation of the mean sun scan values for the two integration techniques show in Fig. 19 (the blue and yellow curves).

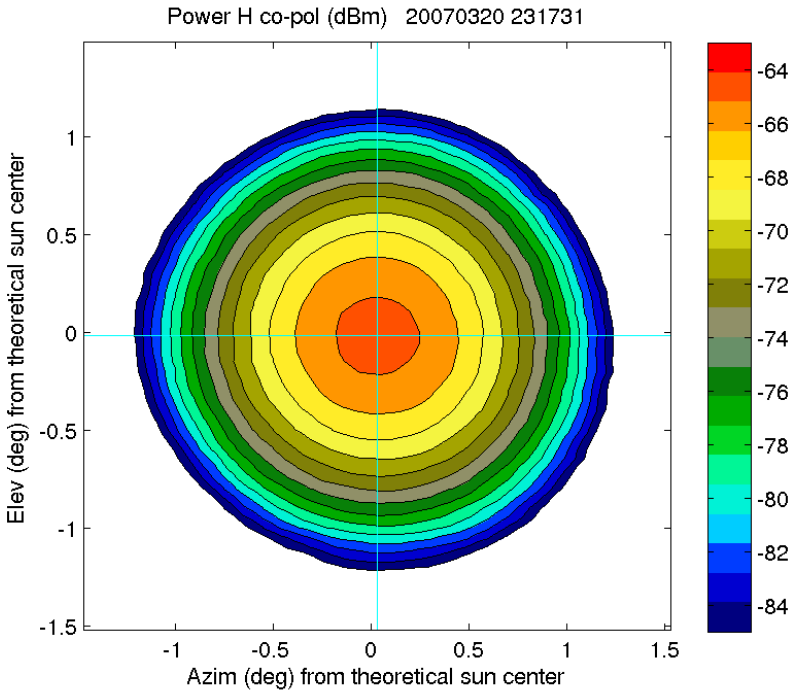

Figure 20: *Pseudo H antenna pattern from sun measurements*

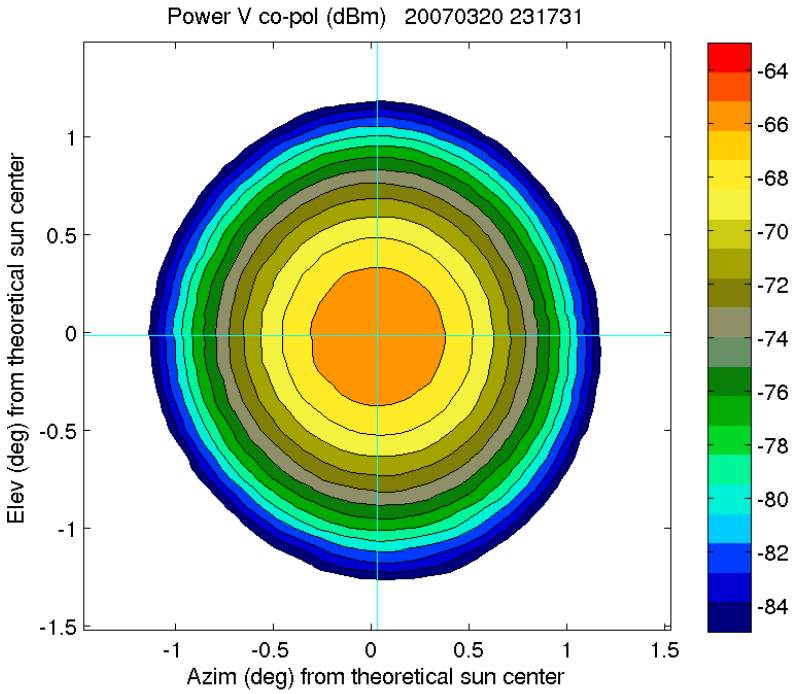

Figure 21: *Pseudo V antenna pattern from sun measurements. Note the vertical elongation along the vertical axis.*

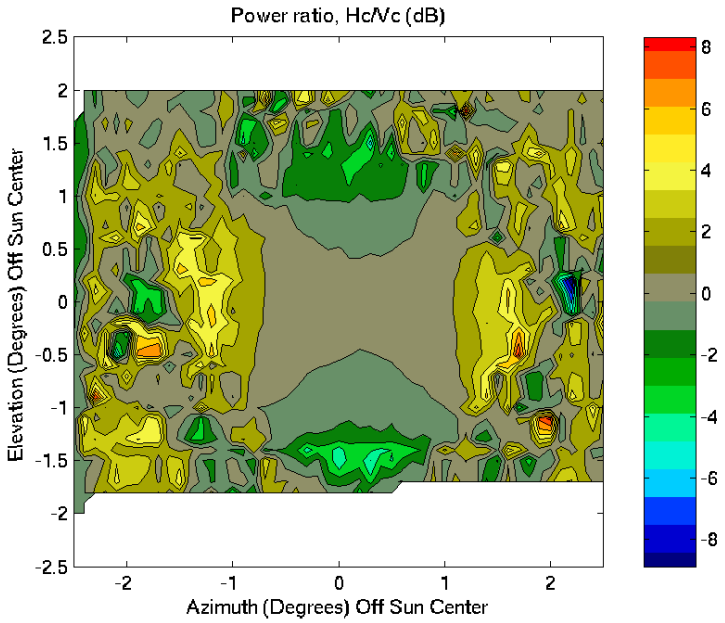

Figure 22: *The ratio of H and V antenna patterns from Figs. 20 and 21.*

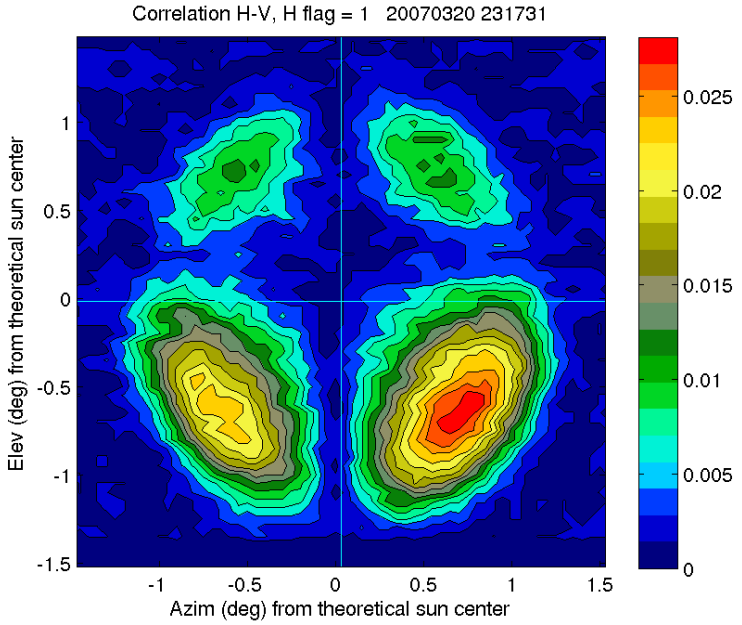

Figure 23: *Correlation between the H and V antenna patterns of Figs. 20 and 21.*

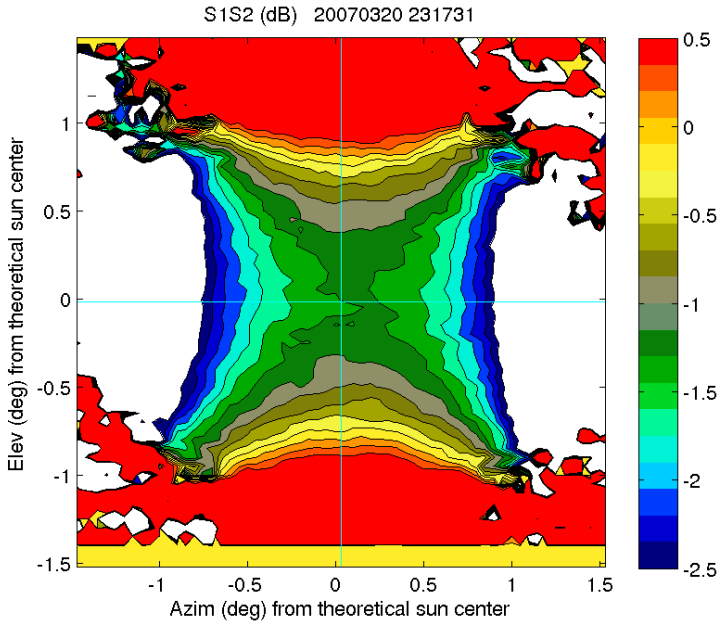

Figure 24: *The ratio S_1S_2 antenna pattern from corresponding to Figs. 20 and 21.*

The FSTDs are found to be about 0.05 dB for the blue data (old integration technique) and 0.02 dB for the yellow data. This then indicates that the griding of the sun scan data and integrating over an annulus does indeed reduce the standard deviation of the S_1S_2 estimates and reduces some of the possible systematic errors associated with the sun integration technique and procedure.

6.2 *Vertical Pointing Measurements*

Vertical pointing measurements in rain have an intrinsic Z_{dr} of 0 dB when data is averaged over a 360° rotation of the radar dish. A measured non-zero value is considered the system Z_{dr} bias. To evaluate the uncertainty of the VP Z_{dr} bias estimate, six consecutive iZ_{dr} bias measurements were made while S-Pol was vertically pointing in light rain on 31 August 2006 using RVP8. Each measurement results from integrating measured Z_{dr} over one 360° antenna revolution and over the range between 2 and 9 km above the radar for data with SNR$>$ 30 dB. The calculated numbers are (in dB):

0.7267 0.7232 0.7210 0.7112 0.6929 0.6726

The mean is 0.712 dB and the standard deviation is 0.019 dB. The 2σ uncertainty of the mean estimate is 0.007 dB.

6.3 *Crosspolar Power Data*

In addition to the sun measurements, the CP technique for Z_{dr} calibration requires the measurement of the mean crosspolar power ratio, $\overline{P_{xv}}/\overline{P_{xh}}$. On 31 August 2006 several volume scans of storms cells were made by S-Pol in fast alternating H and V mode using RVP8. The number of samples per gate was 64 and the scan rate was 12°s^{-1}. Data were averaged over 14 separate PPI scans at elevation angles above

2°. Clutter returns are filtered out by requiring the absolute radial velocity to exceed 2 m s^{-1}. (However, clutter returns can also be used since clutter targets should also be reciprocal scatterers and thus can be used for the Z_{dr} calibrations and this is demonstrated later). The power ratios of $\overline{P_{xv}}/\overline{P_{xh}}$ are, in dB:

-0.312 -0.335 -0.326 -0.341 -0.347 -0.357 -0.347
-0.263 -0.276 -0.304 -0.337 -0.319 -0.343 -0.319

The mean is -0.323 dB and the fractional standard deviation is .026 dB so that the 2σ uncertainty is 0.052 dB for the individual mean estimates. However, the mean estimate of -0.323 dB is more reliable and the 2σ uncertainty is 0.014 dB.

As mentioned before, the NEXRAD dual polarization system will use simultaneous H and V transmission and reception and thus, near simultaneous samples of H and V crosspolar returns will not be available. However, if two slow waveguide switches are used, then the NEXRADs will be able to measure both crosspolar powers. One technique for the evaluation of $\overline{P_{xv}}/\overline{P_{xh}}$ is to alternate between only H and only V transmission on a PPI to PPI basis. If the beams are indexed, crosspolar powers from the same resolution volumes (but from different PPI scans) can be paired and used for the CP calibration. On 18 October 2006 this measurement technique was tested using RVP8 data. Elevation scan data was collected in fast alternating transmit H and V mode, followed shortly by H-only transmit, and then V-only transmit modes. The crosspolar power ratios were calculated from both sets of data. For 22 H and V PPI pairs, the mean crosspolar power ratio is $\overline{P_{xv}}/\overline{P_{xh}} = 0.373$ dB with a 2σ uncertainty of 0.032 dB. Similarly, for the fast alternating mode, the mean $\overline{P_{xv}}/\overline{P_{xh}} = 0.404$ dB and the 2σ uncertainty is 0.002 dB. The uncertainty of $\overline{P_{xv}}/\overline{P_{xh}}$ for the fast alternating method is much lower than that for the alternate H and V PPI method; however, these results suggest that the cross polarization approach is amenable to NEXRAD.

6.4 *Engineering Calibration Results*

Using a combination of Type A evaluations and Type B uncertainty estimates, uncertainty budgets for the 1) NSSL "long" 2-coupler method 2) NCAR single coupler method and 3) the new NSSL "short" are complied in Table 5. The listed uncertainties are 1σ and then the calculated uncertainties are "expanded" to 2σ uncertainty estimates. The left hand column estimates are for laboratory experiments where measurement variables can be very tightly controlled. This degree of precision can not be expected for practical measurements conducted the field. Thus the right hand column gives uncertainty estimates that are for "practical" or operational situations. The 2σ uncertainty of the three EC methods for Z_{dr} bias measurement are about 0.3 dB with the NCAR single-coupler method being the smallest at 0.26 dB.

Part of the uncertainty budget is Type A evaluations. S-Pol has 4 pairs (H,V) of installed waveguide couplers: three pair are located in the transmitter trailer (measurement plane 3 of Fig. 4) and one pair at the antenna port on the elevation arms (measurement plane 2). Having multiple waveguide couplers allows for a redundancy of measurements and therefore a means by which to evaluate measurement uncertainty. RVP8 was used for the three EC approaches tested.

Thus far, four complete manual engineering calibrations have been completed on 4 January, 24 January, 8 February and 16 February, 2007. With the completion of the ATE, the EC calibration can be conducted on the order of 15 minutes rather than the full day required for the manual EC calibration. Thus a much more complete evaluation of the EC technique is now possible and this will be included in future reports. However, regardless of EC method, the uncertainty is well above the 0.1 dB level. also combined using the NSSL-proposed EC approach and the Z_{dr} measurement bias is 0.801 dB with an

Uncertainty Components (Errors)	"The Lab" u in dB	dB^2		"Practical" u in dB	dB^2
ZDR Bias "Double-Coupler" Approach					
"Transmit Power Differential" @ RefPoint2	0.023	0.0006		0.085	0.0073
"Receiver Injection Differential" @RefPoint2	0.012	0.0001		0.043	0.0018
"Receiver Injection Differential" @RefPoint3	0.023	0.0006		0.085	0.0073
"Antenna Gain Differential Error"	0.06	0.0036		0.08	0.0064
"Dynamic Inaccuracy"	0.03	0.0009		0.03	0.0009
"Procedural Error"	0	0		0	0
u combined	*0.076*			*0.154*	
Expanded Uncertainty Uk, k=2 "2-sigma"	***0.151***			***0.307***	
ZDR Bias "Single-Coupler" Approach					
"Transmit Power Differential" @ RefPoint2	0.023	0.0006		0.085	0.0073
"Receiver Injection Differential" @ RefPoint2	0.012	0.0001		0.043	0.0018
"Receiver Injection Differential" @RefPoint3	0	0		0	0
"Antenna Gain Differential Error"	0.06	0.0036		0.08	0.0064
"Dynamic Inaccuracy"	0.03	0.0009		0.03	0.0009
"Procedural Error"	0	0		0	0
u combined	*0.072*			*0.128*	
Expanded Uncertainty Uk, k=2 "2-sigma"	***0.144***			***0.256***	
ZDR Bias "Double-Coupler Simplified" (Dusan's)					
"Transmit Power Differential" @ RefPoint2	0.023	0.0006		0.085	0.0073
"Receiver Injection Differential" @ RefPoint2 ***	0	0		0	0
"Transmit Antenna Gain Differential"	0.06	0.004		0.08	0.006
"Receive Antenna Gain Differential"	0.03	0.0009		0.04	0.0016
"Coupling Factor Calibration Error"	0.04	0.0016		0.05	0.0025
"Coupling Factor" Error Injection Measurement	0	0		0	0
"Dynamic Inaccuracy"	0.03	0.0009		0.03	0.0009
"Procedural Error"	0	0		0	0
u combined	0.087			0.137	
Expanded Uncertainty Uk, k=2 "2-sigma"	**0.174**			**0.273**	

Table 5: *The estimated uncertainty budgets for (from top to bottom) 1) the NSSL 2-coupler of "long" method, 2) the NCAR 1-coupler method and 3) the NSSL new short method.*

uncertainty of 0.302 dB. The details of these measurements are given in Appendix B.

6.5 *Comparison of Z_{dr} Calibration Techniques*

The Z_{dr} calibration factor or bias of the S-Pol system should be the same whether using the vertical pointing (VP), the crosspolar power or engineering techniques. The Z_{dr} bias calculated above from VP data is 0.712 dB$\pm$0.019 dB. The Z_{dr} bias can also be calculated via the CP technique using Eq.(15) from sun measurements and crosspolar power measurements, also gathered on 31 August 2006. S_1S_2 was found to be -1.051 dB$\pm$0.013 dB while the crosspolar power ratio was -0.323 dB$\pm$0.014 dB. This yields a Z_{dr} bias of $(-0.323) - (-1.051) = 0.728$ dB$\pm$0.027 dB which is in excellent agreement with the VP bias estimate 0.712 dB$\pm$0.019 dB. Both of these uncertainties are derived from Type A evaluations. There are likely other Type B, systematic errors that we have neglected for both techniques. For the VP method we estimate a Type B uncertainty of 0.05 dB. For the CP technique, we estimate a Type B uncertainty of 0.05 dB for both the crosspolar power ratio $\overline{P_{xv}}/\overline{P_{xh}}$ and the sun ratio measurement S_1S_2. This then changes the VP bias estimate to 0.712 dB$\pm$0.053 dB and the the CP estimate to 0.728 dB$\pm$0.075 dB. Both 2σ uncertainties are still under the 0.1 dB requirement. The results from the EC approach indicate Z_{dr} measurement bias is 0.80 dB with a total uncertainty of about 0.25 dB (other uncertainties are included in this estimate that were not included in Section 3.5 above. The EC bias number of 0.80 dB was estimated from data taken over several days so that a direct comparison of the EC bias to the CP and VP biases is not warranted. The uncertainty estimate of the EC bias, 0.25 dB, however, more importantly indicates that the EC Z_{dr} bias may not be estimated to within the 0.1 dB requirement. More data sets need to be gathered to confirm these numbers.

7 SUMMARY AND CONCLUSIONS

NCAR is conducting an experiment for OS&T of NOAA/NWS to evaluate Z_{dr}calibration techniques for the WSR-88Ds using S-Pol, NCAR's S-band polarimetric radar. Three techniques for Z_{dr} calibration were investigated: 1) vertical pointing data in light rain, 2) engineering calibration technique and 3) the crosspolar power technique. Measurement and analyses were performed in order to quantify the uncertainty of the estimated calibration numbers and the measurement procedures that yield such uncertainty. The uncertainty of measurements can be separated into two categories: 1) systematic and 2) random. Random errors can be reduced by averaging,where as systematic error can not. Uncertainty can be quantified by Type A evaluations, i.e. repeated trials under controlled test conditions, and by Type B evaluations which can be defined as any other error quantification method other than Type A. For example, manufacture specifications are Type B evaluations or errors.

Vertical pointing (VP) measurements in light rain are widely regarded as the most accepted way to calibrate Z_{dr} and such measurements were used to truth other Z_{dr} calibration measurements. Several sets of vertical pointing data were gathered over the the summer of 2006 and analysis showed that the Type A uncertainty of the vertical point Z_{dr} calibration was on the order of 0.01 dB. Again, this is an evaluation of the *random measurement errors* and possible systematic biases may be present, e.g. due to data processing.

A main objective of this Z_{dr} calibration experiment was to establish the uncertainty of the NSSL EC technique though three other EC techniques were evaluated: 1) the new NSSL "short" EC method, 2) the S-Pol legacy method (based on the radar equation) and 3) the NCAR one-coupler method. The uncertainty of the EC techniques were established via both Type A and Type B uncertainty evaluations. The results reported are preliminary and the uncertainty should improve as the measurement methods

are improved. Using average S-Pol engineering measurements taken during summer 2006 and combined through the weather radar equation, termed the S-Pol legacy approach, Z_{dr} measurement bias was calculated to be 0.640 dB with an uncertainty of 0.319 dB. The S-Pol legacy calibration was performed as an initial systems evaluation and was used for comparative purposes. Since then, four complete manual EC calibrations have been completed. The measurements were combined using the NSSL-proposed 2-coupler approach, the NSSL short approach and the NCAR one-coupler method. The Z_{dr} measurement bias was about 0.840 dB for both the NSSL two-coupler and NCAR methods. The bias for the NSSL short method was about 1 dB, which is a higher value than indicated by all other techniques. The accompanying Type A evaluations were combined with Type B uncertainty evaluation to arrive at overall uncertainty budgets. The 2σ uncertainties calculated are: 0.307 dB for the NSSL 2-coupler method, 0.256 dB for the NCAR short method and 0.273 dB for the NSSL short method. A large component of these uncertainty numbers is due to impedance mismatches.

Evaluation of sun measurements impacts both the engineering calibration technique (EC) as well as the crosspolar power technique (CP). The sun's radiation (at S-band) can be considered unpolarized and thus the power of the sun is equally divided between horizontal (H) and vertical (V) polarizations. Sun flairs can create polarized radiation but is typically considered circularly polarized which also provides equal powers between the H and V channels. Thus, the sun's radiation is an excellent RF source for the evaluation of the differential gain of a a radar's H and V receive channels.

Analysis of sun measurements showed that about 500,000 samples (I and Q measurements) of the sun are required to reduce the mean estimate of the sun's power to an uncertainty of about 0.01 dB. For the S-Pol system that uses a switch at the IF stage to create copolar and crosspolar receivers, there are two sun power ratios required for the CP calibration technique, namely S_1 and S_2. It is the product of these two ratios that appears in the calibration equation Eq.(15). Analysis of data sets of the S_1S_2 product gathered over about 0.5 hour yield a fractional uncertainty of 0.0041 dB. From 14 June to 24 August 309 solar box scans were made and a long term analysis of S_1 and S_2 from this data set yielded an uncertainty of 0.049 dB (2σ). These are Type A uncertainty evaluations. Possible systematic errors are also possible present (and undetected). One source of systematic error is the integration technique used to calculate S_1S_2. A more sophisticated method for integration of the sun data was given that used a griding technique and it was shown to reduce this possible error source. Even though our Type A evaluation show very low variance, during high sun spot activity the power across the sun may become variable enough to change the weighting of the antenna patterns and thus cause additional systematic errors.

Measurements with S-Pol thus far show excellent agreement between the Z_{dr} bias found via VP measurements and the CP techniques (biases of 0.712 dB and 0.728 dB, respectively). For the experimental data used here, both techniques yielded uncertainties well within the desired uncertainty limit of 0.1 dB. Additionally, it was shown that the crosspolar power technique can be successfully employed on radar systems that achieve dual polarization measurement via simultaneous transmission of H and V polarizations as NEXRAD will do. In this case, slow waveguide switches were used to gather alternate PPIs of transmit only H and transmit only V data. Using indexed beams, the transmit H and transmit V crosspolar powers from the alternate PPIs were equated. This can done for ground clutter since the backscatter cross sections of stationary ground clutter targets is invariant. These results indicate that the crosspolar technique could be used with NEXRAD type radars.

Further evaluation of the engineering calibration technique will now be possible with the recently completed Automated Test Equipment (ATE) system. The success of the engineering calibration technique will depend in part on precise measurement of the specifications for the waveguide couplers. The impedance mis-matches between the various connections will also need to be accounted for if Z_{dr} is to be calibrated to within 0.1 dB uncertainty. Data sets where all three Z_{dr} calibration techniques can be

executed in close temporal proximity (with a half hour) are needed. See Section B.5 of the Appendix for EC calibration observations and recommendations.

Acknowledgment
This work was supported by NOAA's National Weather Service Office of Science and Technology. The authors would like to acknowledge the EOL/RSF technical staff for their time, effort and interest in the collection of the experimental data used in this report.

References

Bringi, V. and V. Chandrasekar, 2001: *Polarimetric Doppler Weather Radar*. Cambridge Univ. Press, Cambridge, UK.

Doviak, R., V. Bringi, A. Ryzhkov, A. Zahrai, and D. Zrnić, 2000: Polarimetric upgrades to operational WSR-88D radars. *J. Atmos. Oceanic Technol.*, **17**, 257–278.

Hubbert, J., F. Pratte, M. Dixon, R. Rilling, and S. Ellis: 2006, Calibration of Z_{dr} for NEXRAD. *IGARSS-2006*, Denver, CO.

Hubbert, J. and V.N. Bringi, L.D. Carey, and S. Bolen, 1998: CSU-CHILL polarimetric radar measurements in a severe hail storm in eastern Colorado. *J. App. Meteor.*, **37**, 749–775.

Hubbert, J.C., V.N. Bringi and D. Brunkow, 2003: Studies of the polarimetric covariance matrix: Part I: Calibration methodology. *J. Atmos. and Oceanic Technol.*, **20**, 696–706.

Jursa, A.S. (Editor) , 1985: *Handbook of Geophysics and the Space Environment*. National Technical Information Service, iSpringfield , VA, 4 edition.

Kearn, D. and R. Beatty, 1967: *Basic Theory of Waveguide Junctions and Introductory Microwave Analysis*. Pergamom Press.

Keeler, R., J. Lutz, and J. Vivekanandan: 2000, S-POL: NCAR's polarimetric Doppler research radar. *IGARSS-2000*, Honolulu, Hawaii.

Kraus, J.D. , 1986: *Radio Astronomy,*. Cygnus-Quasar Books, 2^{nd} edition.

Saxon, D.S., 1955: Tensor scattering matrix for the electromagnetic field. *Phys. Rev.*, **100**, 1771–1775.

Tapping, K.: 2001, Antenna calibration using the 10.7 cm solar flux. *Radar Polarimetry for geoscience applications*, P. Smith, ed., American Meteorological Society, http://cdserver.ametsoc.org/cd/010430_1/RADCAL_Links_2_Presentations.html.

Taylor, J., 1997: *An Introduction to Error Analysis*. University Science Books, Sausalito, CA.

Taylor, B.N., and C.E. Kuyatt, 1994: Guidelines for evaluating and expressing the uncertainty of NIST measurements results. Technical report, US Dept. of Comm. National Institute of Standards and Tech., note 1297.

Technologies, A., 2001: Fundamentals of rf and microwave power measurements. Technical report, Agilent Technologies, application Note 64-1C.

Zrnić, D.S., V.M. Melnikov, and J.K. Carter, 2006: Calibrating differential reflectivity on the WSR-88D. *J. Atmos. and Ocean. Tech.*, **23**, 944–951.

Uncertainty	dB V	dB P
-25.0%	-2.499	-1.249
-10.0%	-0.915	-0.458
-5.0%	-0.446	-0.223
-1.0%	-0.087	-0.044
-0.5%	-0.044	-0.022
0.5%	0.043	0.022
1.0%	0.086	0.043
5.0%	0.424	0.212
10.0%	0.828	0.414
25.0%	1.938	0.969

Table A1: *The voltage and power decibel values for various percent uncertainties.*

k	Normal Containment	Normal Exclusion
0.500	38.29%	61.71%
0.675	50.03%	49.97%
1.000	68.27%	31.73%
2.000	95.45%	4.55%
3.000	99.73%	0.27%
4.000	99.99%	0.01%

Table A2: *The coverage factor k and the Normal distribution.*

APPENDIX

A THE QUANTIFICATION OF UNCERTAINTY

RF quantities are often expressed as ratios in decibels, but uncertainties are dealt with as linear quantities. When interpreting uncertainties from manufacturers specifications it is instructive to note how small variations in quantities expressed as percentages from the mean or expected values. Things to note are that the decibel notation is not symmetric about the mean. As a reference, 5% is approximately 0.2 dB and 1% is approximately 0.05 dB (using power). One dB is equivalent to about 25% in power or 12% in voltage. For reference, Table A1 shows the dB voltage and dB power values for various percent levels of uncertainty.

Uncertainty (or accuracy, or nominal error, in times past) of measurements is a recognized measure of dispersion. Many commercial specifications are given with 95% confidence (2σ) as limits or percentages based on a normally-distributed uncertainty model. Specifying a model and a coverage factor quantifies confidence in the specification. We will use that here unless otherwise noted. Table A2 lists coverage factors (k) with the corresponding percentages contained within limits of +/- k times the standard deviation, and the percentage outside the limits.

A.1 *Uncertainty Calculations*

The mean of a data set $x(i)$ is

$$\mu = \frac{1}{N}\sum_{i=1}^{N} x(i) \tag{A1}$$

and the standard deviation is

$$\sigma = \sqrt{\frac{1}{N-1}\sum_{i=1}^{N}(x(i)-\mu)^2} \tag{A2}$$

The fractional uncertainty is defined as

$$F_u = \sigma/\mu \tag{A3}$$

To convert fractional uncertainty to decibel scale,

$$F_u(dB) = 10\log_{10}\{1+F_u\} \tag{A4}$$

Thus the fractional uncertainty of a single measurement $x(i)$, taken under the identical conditions as that of the data set, is F_u. However the uncertainty of the estimated mean μ of the data set is (in dB)

$$F_u(\mu) = \frac{10\log_{10}\{1+F_u\}}{\sqrt{N}} \tag{A5}$$

where N is the number of measurements in the data set. As is seen, the uncertainty of the measured mean of a data set is reduced as the number of measurements increases. This is referred to as the standard deviation of the mean (SDOM) and is also expressed as

$$\sigma_{\bar{x}} = \frac{\sigma_x}{\sqrt{N}}. \tag{A6}$$

The following equations demonstrate how uncertainties are combined for random and independent errors.

Sums and Differences: If

$$q = x + y + z \tag{A7}$$

then

$$\delta q = \sqrt{(\delta x)^2 + (\delta y)^2 + (\delta z)^2} \tag{A8}$$

i.e., the total uncertainty (δq) of a measurement q that is composed of the sum of three measurements x, y and z, is the quadrature sum of the individual uncertainties, δx, δy, δz.

Products and Quotients: If

$$q = \frac{x \times y \times z}{u \times v \times w} \tag{A9}$$

then

$$\delta q = \sqrt{\left(\frac{\delta x}{x}\right)^2 + \left(\frac{\delta y}{y}\right)^2 + \left(\frac{\delta z}{z}\right)^2 + \left(\frac{\delta u}{u}\right)^2 + \left(\frac{\delta v}{v}\right)^2 + \left(\frac{\delta w}{w}\right)^2} \tag{A10}$$

i.e., the total uncertainty of a measurement q that is composed of the product of the measurements x, y, z, u, v, and w is the quadrature sum of the individual *fractional* uncertainties.

If the errors are not independent, an upper bound on the uncertainty can be obtained by simple addition of the individual error terms. The quadrature sum is always less than or equally to the algebraic sum, i.e., it can be shown for Eq. (A10), for example, that

$$\delta q \leq \frac{\delta x}{|x|} + \frac{\delta y}{|y|} + \frac{\delta z}{|z|} + \frac{\delta u}{|u|} + \frac{\delta v}{|v|} + \frac{\delta w}{|w|} \tag{A11}$$

For the uncertainty budgets presented in this report, individual uncertainties are combined using the product-quotient rule of Eq. (A10), i.e., the errors are assumed uncorrelated.

Finally, the fractional uncertainty of a calculated standard deviation, σ_x, is

$$\text{fractional uncertainty in } \sigma_x = \frac{1}{\sqrt{2(N-1)}} \tag{A12}$$

For further details of error analysis, see Taylor (1997).

B MICROWAVE POWER MEASUREMENT EXPERIMENTS

In this appendix additional details concerning the Engineering Calibration technique are given. These measurements follow the NOAA/NSSL-proposed approach as outlined by Zrnić, et al (2006), and were described in an earlier section. Preliminary EC uncertainty budgets are given for the both the NOAA-proposed approach and the customary S-Pol (Keeler et al. 2000) approach used at NCAR. Both suggest an expanded uncertainty (i.e., 2σ coverage) of approximately 0.3 dB. Described are several ongoing experiments conducted on NCAR's S-Pol dual polarization weather radar to deduce power measurement uncertainty components through repeated measurements (Type A methods) and otherwise indirect methods (Type B methods). The goal is to produce a practical uncertainty budget for the various EC methods.

B.1 *Uncertainty of Engineering Calibration of Z_{dr} Bias*

Systematic engineering calibration to determine the Z_{dr} instrument bias, a derived quantity, depends on a set of carefully executed microwave power measurements. From Taylor and Kuyatt (1994), the output quantity's estimate y of desired measurand Y (Z_{dr} measurement bias, in this case) is formed using N input estimates x_i

$$y = f(x_1, x_2, ..., x_n) \tag{B13}$$

The combined standard uncertainty of the measurement result y, designated by $u_c(y)$, taken to represent the estimated standard deviation of the result, is the square root of the estimated variance

$$u_c^2(y) = \sum_{i=1}^{N} (df/dx_i)^2 u^2(x_i) + 2 \sum_{i=1}^{N-1} \sum_{j=i+1}^{N} (df/dx_i)(df/dx_j) u(x_{i,} x_j) \tag{B14}$$

The derivatives are partial (referred to as sensitivity coefficients) and are evaluated at x_i; $u(x_i)$ is the standard uncertainty associated with the input estimate x_i; and $u(x_i, x_j)$ is the estimated covariance associated with input quantities x_i and x_j.

Sample standard deviation will be used as standard uncertainty, approximately normal distributions of summary effects will be assumed, and no attention will be paid to degrees of freedom in this evaluation. (The initial approximation for small sample sizes is reasonable as with 10 degrees of freedom, the coverage factor for 95% coverage increases (Student) by only 14% from that of a normal distribution). Selection of uncertainty components is ultimately based on experience, research into experimental incongruities, literature, and engineering judgment.

a) NOAA-proposed EC Approach A functional relationship among the individual power measurements x_i and the derived estimate y can be obtained directly from the polarimetric radar system diagram given previously in Fig. 4. Simultaneous power measurements are made at five microwave power test planes (including the sun) in each of the two polarization channels as shown in Fig. 4. Reference plane 1 is physically located inside the radar shelter at the transmitter output waveguide. Reference plane 2 is located in waveguide at the antenna flanges and downstream (transmit direction) from the transmit-receive circulators and pedestal rotary joints. Reference plane 3 (blue) is an extra measurement point located near the antenna ports of the circulators. Reference plane 3' (green) is found downstream (receive direction) from the circulators and before the low noise amplifier. Finally, reference plane 4 is the digital readout after the intermediate frequency digitizers following the analog portion of the receiver. Pairs of path gain

measurements are made in two groups. The first group measures the gain (or loss) ratio (difference in decibels) between reference planes 1 and 2. The second between 2 and the antenna far field (reference plane S), the third between reference plane 2 and plane 3', and finally between 3' and 4.

Z_{dr} measurement bias formula (error terms not shown) obtained from the NOAA-proposed approach given in Zrnić et al. (2006) is given in decibel notation as follows with eight input quantities

$$M_{bias}(k) = \Delta(1,2,k)_{pulse} + 2[\Delta(S,4,k)_{noise} - \Delta(3,4,k)_{noise} - \Delta(2,4,k)_{cw} + \Delta(3,4,k)_{cw}] \\ +\Delta(2,4,k)_{cw} - \Delta(3,4,k)_{cw} + \Delta(3,4,k)_{cw\_operate} \quad \text{(B15)}$$

In this equation M_{bias} is the desired measurement bias estimate, the "Δs" are gain ratios of the passive or active components in the transmit, antenna, and receive paths. For example, $\Delta(3,4,k)_{cw\_operate}$ is the gain ratio of the active components in the receive path derived from online measurements (every 10 minutes or so) and thus contains automatic adjustment for receive path drifts. Other Δs are considered system constants and those gain ratios are identified with the following measurements:

$\Delta(1,2,k)_{pulse}$: Transmitter top of frame to antenna port which yields average differential readings in decibels on power meter of pulse power from transmitter to antenna coupler. Conducted to minimize power meter setup variations and drifts.

$\Delta(3,4,k)_{noise}$: Response to noise injection through receive path (LNA) couplers to digitizers, assumed conducted in a way that corrects for background noise, RF leakage, and RF interference.

$\Delta(3,4,k)_{cw}$: Response to continuous wave (CW) injection, measured gain ratio from receiver (LNA) couplers to digitizers, also assumed conducted in a way that corrects for background noise, RF leakage, and RF interference and consistent, if not identical, to existing WSR-88D online calibration adjustments during system operation.

$\Delta(2,4,k)_{cw}$: Response to CW injection, measured gain ratio from antenna couplers to digitizers, assumed conducted in a way that corrects for background noise, RF leakage and RF interference.

$\Delta(S,4,k)$: Gain ratio from far-field solar injection to IF digitizers also assumed conducted in a way that corrects for background noise, RF leakage, and RF interference, and source variability (impulsive solar RF bursts, non-uniform illumination, etc), and assumed that transmission ratio of H and V polarized waves from sun to radome is unity. The radome is measured as part of the antenna system.

The path gain ratios are obtained by calculation from the results of pairs of simultaneous microwave power measurements at each plane. At each reference plane the sidearm ports of the S-band waveguide couplers provide the measurement points, save for plane 4 where the voltage across a known load at intermediate frequency is sampled and then squared. Three signal waveforms are used in the calibration process. Pulsed RF from the transmitter source is used for the 1,2 gain ratio. Noise from solar emissions is the signal for the 2,3 gain ratio, and narrowband continuous wave (CW) is the calibration signal used for the 3,4 gain ratio calculations. Note that the physical location of the transmit subsystem reference 2 and receiver subsystem reference 3 are different so an effective translation of reference planes occurs in the functional formula. Parameter k is used as a reminder of the "power step" or "power level" being measured and the implication of differential linearity. The subscripts cw, noise, and pulse serve as a reminder of signal modulation during measurements. Numerical references are indicated to measurement planes described above. The formula does not specifically include splitter, coupler, and mismatch error terms which depend on the scattering parameters of the waveguide junctions used in the measurements. Nor

does the formula show background noise correction terms, nor factors for effect of different H and V beam asymmetries that may arise when viewing beam-filling distributed targets. Each measured power needs to be corrected for the background noise of that trial and we also assume that the pairs are simultaneous or at least contiguous in time.

b) The S-Pol EC Approach The customary (legacy) S-Pol EC approach obtains the Z_{dr} bias estimate M_{bias} from the calibrated quantities used in the weather radar equations. The formula for Mbias is obtained from the reflectivity ratio Z_H/Z_V and simplifies to the following in decibel notation (error terms not shown)

$$M_{bias}(k) = (P_t^H - P_t^V) + (2G_s^H - 2G_s^V) + (\Theta_H - \Theta_V) + (\Phi_H - \Phi_V) - (G_r^H(k)x - G_r^V(k)). \quad \text{(B16)}$$

The input quantities P_t, G_s, Θ, Φ, and G_r are obtained for H and V channels referenced at a measurement point. P_t is peak transmit power, G_s the antenna system gain, Θ and Φ main beam widths and G_r is the receiver and digitizer gain of the lower or higher magnitude receiver (k).

For the WSR-88D dual-polarized antenna, beamwidths (Θ, Φ) and gains (G_s) will be related by a formula of the following type in decibel notation

$$G_s^H - G_s^V = \Theta_V + \Phi_V - -\Theta_H - -\Phi_H + k_g^H - k_g^V \quad \text{(B17)}$$

Where k_g is a gain coefficient dependent on the antenna illumination function and system losses. Thus there will be inverse correlation between the gains and beamwidths.

c) Preliminary Z_{dr} Bias Uncertainty Budgets Preliminary uncertainty budgets have been developed for the EC approach customarily used at S-Pol (S-Pol legacy approach) and the NOAA-proposed approach. The first column in the following budgets contain mean ratios and uncertainty estimates for components summarized as from Type A and Type B methods in each listed category at each radar signal measurement point. For a single round of measurements on one radar the variations determined by Type A methods for this budget may be interpreted in the classical sense as the random errors and by Type B methods as the bias errors. Component uncertainties in each type category were estimated in decibels. Linear units were used to calculate the combined standard uncertainty in this simplified budget as the root-sum-squares measure of the eight component numbers (2). Mean ratio for beamwidth has not been determined, so is set to zero. The mean ratios are then combined according to (3) or (5) to arrive at the derived quantity M_{bias} shown at the bottom of the column. Ratio values are expressed in decibels and in linear units in the adjacent columns.

Although the combined standard uncertainty u_c can be used to express the uncertainty of measurement results, for commercial, industrial, and regulatory applications what is required is an interval about the derived result y within which the value of the measurand Y is *confidently* believed to lie. The measure of uncertainty intended to meet this requirement is termed "expanded uncertainty" (Taylor and Kuyatt 1994), and is obtained by multiplying $u_c(y)$ by coverage factor k and by assuming that the deviations are normally distributed. Therefore $U = ku_c(y)$, and it is confidently believed that $y - U \leq Y \leq y + U$, which is commonly written as

$Y = y \pm U$. To be consistent with current international and engineering practice, the value of k to be used at for calculating U is, by convention, $k = 2$ and approximates the 95% level of confidence.

Uncertainty Evaluation of Zdr Measurement Bias Mbias (Preliminary)
S-Pol's Customary (Legacy) Engineering Calibration (EC) Approach, S-Pol Experiments
(Based on RVP8 and waveguide RF power measurements, summer 2006)

	H/V dB	H/V Linear
PtH, PtV Transmit Power Ratio		
Pt ratio dB for Mbias calculation	0.15	1.04
Estimate u dB Type A	0.02	0.00
Estimate u dB Type B	0.11	0.03
GaH, GaV, Antenna System Gain Ratio		
Gs ratio dB for Mbias calculation	0.41	1.10
Estimate u dB Type A	0.02	0.00
Estimate u dB Type B	0.04	0.01
GHc, GVc Receiver Gain Ratio		
Gr ratio dB for Mbias calculation	0.33	1.08
Estimate u dB Type A	0.02	0.00
Estimate u dB Type B	0.04	0.01
ThetaH, ThetaV Beamwidth Ratio		
Theta ratio dB for Mbias calculation	0.00	1.00
Phi ratio dB for Mbias calculation	0.00	1.00
Estimate u dB Type A	0.03	0.01
Estimate u dB Type B	0.05	0.01
S-Pol ZDR Measurement Mbias dB	**0.640**	
Combined Standard uc (assume uncorrelated components)	**0.162**	0.038
Coverage Factor k		2.000
Expanded Uk	**0.319**	0.076

Table B3: *Evaluating S-Pol's Z_{dr} measurement bias from subsystem average measurements by S-Pol's customary (legacy) approach. From measurements taken during summer 2006 we find a preliminary Mbias estimate of 0.640 dB and its expanded uncertainty of ± 0.319 dB (extra digits not particularly meaningful, but retained for reader orientation).*

Since the experimental campaign and analyses have not completed, there is some uncertainty as to which error components dominate, their magnitude, and their correlation. They are, however, based on available experimental results, what we know of the performance of modern weather radars, our experience with the WSR-88D, and the remainder on engineering experience. At this interim, the combined standard uncertainty was evaluated using Eq. (B14) assuming that the components are uncorrelated, as is frequently the case early in evaluations. These uncertainty budgets, given in Tables B3 and B4 do, however, represent a very reasonable estimates of the likely final EC uncertainties.

B.2 *Experimental Approach*

Contributors to microwave power measurement uncertainty are operating wavelength, uncertainty of waveguide coupling factor (coupler scattering parameters), effective reflection coefficients of coupler and sensor assemblies (including attenuators and adapters), power meter uncertainties in absolute and differential modes, connector and cable repeatability, source amplitude variation and source modulation, ambient temperature drift, and ambient humidity fluctuations, component heating, return loss of the main waveguide runs, procedural variations, and non-linear behavior of digitizers and power meters. At the outset we suspect that impedance mismatch issues will be a dominant component at the 0.1 dB level, even though good test equipment, cables, attenuators, and connectors are used. These are related to generally unknown waveguide junction scattering parameters and reflection coefficients of forward and reverse paths from each measurement.

Uncertainty Evaluation of Zdr Measurement Bias Mbias (Preliminary)
NOAA-Proposed Engineering Calibration (EC) Approach, S-Pol Experiments
(Based on RVP8 and waveguide RF power measurements, summer 2006)

	H/V dB	H/V Linear
PtH, PtV Transmit Power Ratio Delta (1,2,k)pulse		
Pt ratio dB for Mbias calculation	1.64	1.46
Estimate u dB Type A	0.01	0.00
Estimate u dB Type B	0.09	0.02
GaH, GaV, Antenna System Gain Ratio Delta(S,4,k)noise		
Gs ratio dB for Mbias calculation	0.53	1.13
Estimate u dB Type A	0.01	0.00
Estimate u dB Type B	0.04	0.01
GHc, GVc Receiver Gain Ratio Delta(3,4,k)noise		
Gr ratio dB for Mbias calculation	-0.35	0.92
Estimate u dB Type A	0.01	0.00
Estimate u dB Type B	0.03	0.01
GHc, GVc Receiver Gain Ratio Delta(2,4,k)cw		
Gr ratio dB for Mbias calculation	1.85	1.53
Estimate u dB Type A	0.01	0.00
Estimate u dB Type B	0.03	0.01
GHc, GVc Receiver Gain Ratio Delta(3,4,k)cw		
Gr ratio dB for Mbias calculation	-0.37	0.92
Estimate u dB Type A	0.01	0.00
Estimate u dB Type B	0.03	0.01
ThetaH, ThetaV Beamwidth Ratio		
Theta ratio dB for Mbias calculcation	0.00	1.00
Phi ratio dB for calcs	0.00	1.00
Estimate u dB Type A	0.03	0.01
Estimate u dB Type B	0.05	0.01
S-Pol ZDR Measurement Mbias dB	**0.801**	
Combined Standard uc (assume uncorrelated components)	**0.154**	0.036
Coverage Factor k		2.000
Expanded Uk	**0.303**	0.072

Table B4: *Evaluating S-Pol's Z_{dr} bias using subsystem average measurements by the NOAA-proposed approach. From measurements taken during summer 2006 and the NOAA-proposed formula we find a preliminary Mbias estimate of 0.801 dB and its expanded uncertainty ±0.303 dB (extra digits not particularly meaningful, but retained for reader orientation).*

For power ratio measurements, some errors are highly correlated and these must be distinguished. The correlation of errors can be beneficial as procedures can then be devised to cancel a portion of systematic error. If conducted correctly, differential or ratio measurements are accompanied by less uncertainty than absolute measurements.

In analyzing power measurements the following iterative sequence is used: (1) establish a radar test configuration; (2) develop an error model; (3) develop statistical estimates; and (4) develop an uncertainty budget. Uncertainty budgets are useful in the design of system upgrades, and can help identify rogue measurements later in system life. For step (1) we modified the S-Pol waveguide configuration to mimic the WSR-88D waveguide and receiver configuration, plus we are adding a high-stability measurement/calibration sub-system called ATE (Automated Test Equipment) to maintain a high stability reference spanning the time between vertical pointing (VP) reference measurements, producing our "baseline" bias estimate. We assume that these selective modifications to S-Pol will be adequate to compare approaches statistically. Additionally, we modified the customary S-Pol calibration procedures to accommodate additional experimental results for validating the NOAA-proposed approach.

For step (3) "develop statistical estimates" the following types of experiments are being conducted, some in the laboratory, while others in situ on the test radar:

1. Waveguide microwave power measurements emphasizing our metrology concerns.
2. Gain ratio measurements in situ,
3. Uncertainty of coaxial connections.
4. Uncertainty of antenna gain ratio and beamwidth ratio using the sun.
5. Environmental effects on subsystem gains (losses).
6. Monte Carlo modeling of mismatch errors and system equation.
7. Experimental measurements of mismatch errors.
8. Effects of signal and filter bandwidth ratios and frequency offsets.
9. Temperature coefficients of generators and power measuring instruments.
10. Temperature coefficients of receivers and IF digitizer channels.
11. Comparison of vector and scalar power measurements.
12. Differential receiver tracking over extended dynamic range.
13. Effect of variations in making the measurements.
14. Experimental evaluation of legacy S-Pol Z_{dr} calibration procedure.
15. Experimental evaluation of NOAA-proposed Z_{dr} calibration procedure.
16. Measurement of scattering parameters of system components.

B.3 *Influence Factors*

Influences by environmental forcing can explain additional uncertainty components (error sources) of 0.01 dB to 0.5 dB, depending upon conditions. This list can be employed in the design of component tests.

Thermal stress (material expansion, amplifier gain change)

Mechanical Stress (wear out, connector repeatability, cable flex)

Chemical stress (oxidation, dirt)

Moisture (sneak current paths)

Source stability

Modulation (detector response)

RF Interference (nearby RF emitters, isolation)

Procedural (operator bias, computation and recording)

Magnitudes of environmentally forced measurement uncertainties may be found in literature or by experiments on the following pertinent assemblies or sources.

Power sensors

Attenuators

Cables and Power Splitters

Connectors

Waveguide Couplers

Mismatch Coefficients

Solar flux

Amplifiers

CW generators

Noise generators

Preliminary estimates of the temperature coefficients of gain and gain ratio of the S-Pol receiver and digitizer are reported here. In response to long-term shelter temperature variations caused by space cooling (HVAC) equipment, the digitizer power readout and ambient temperature were recorded. The CW generator was a synthesized Hewlett Packard 8672A signal generator, and the noise generator a temperature-stabilized Micronetics NMA-2413. The five-second averages of received power have a calculated standard deviation of approximately 0.002dB on the noise signal. The CW source plus receiver/digitizer chain exhibited a 0.07 dB power variation over a 7 degree F ambient temperature swing

during the typical 1 hour HVAC cycling period. The ratio of copolar received CW powers (Hc/Vc) exhibited a 0.002 dB swing and the ratio of copolar to cross-polar receivers (Hc/Vx) exhibited 0.004 dB change over the same ambient temperature range. These gain and gain ratio variations with temperature are smaller than expected. The notation Hc, Vc, Hx, or Vx denotes the four switched receiver paths in S-Pol, colloquially termed copolar (c) pairs and crosspolar (x) pairs The ratio Hc/Vx conveys the performance of a non-switched receiver.

The temperature-stabilized noise generator showed a 0.04 dB variation over the same 7 degree F ambient temperature swing. The receive noise power ratio Hc/Vc change was 0.02 dB over the temperature swing, a value which exceeds the variation expected. However, the variation of the ratio Hc/Vx was 0.004 dB for the same temperature swing, same as the CW gain ratio variation. As yet the observed change in Hc/Vc is unexplained.

B.4 *Uncertainty of Practical Waveguide Power Measurements*

For power measurements in waveguide the measurand is the power of the forward propagating wave as shown in Fig. 25. The ten uncertainty components shown may be termed (1) directivity error, (2) coupling factor error, (3,4) mismatch error, (5) attenuator through error, (6) sensor error, (7,8) repeat connection error, (9) reference stability error, (10) power meter error. Most of these become constant errors in a power ratio measurement. Expanded uncertainty of microwave power measurement in the field are approximately 0.2 dB for absolute power, 0.1 dB for ratio measurements, and finally 0.05dB for ratio measurements if the coupler factor are known exactly. Table B5 gives the uncertainty budget for waveguide power measurement in circuit in the field, using typical test equipment and assuming good match conditions.

The following are additional assumptions that apply to the uncertainty budget of Table B5 Some have, and others have not, been verified experimentally.

1. Reciprocity at the measurement points hold to an equivalent return loss of -20 dB.
2. All unknown reflection coefficients are equivalent to a maximum VSWR of 1.1.
3. All residual components are uncorrelated (in practice they may be beneficially or unfortunately correlated).
4. For power meters, the calibration factor usually includes both the effective efficiency of the sensor and its mismatch loss. These effects are treated separately in this budget.
5. Channel to channel isolation is at least -30 dB.
6. Typical test equipment is assumed.
7. Rotary joints are assumed to exhibit maximum 0.05 dB wow over 360 mechanical degrees.
8. Circulator is assumed to provide maximum VSWR 1.1 at any port, whether transmit or receive.
9. Waveguide couplers are assumed to possess maximum VSWR 1.1 at sidearm and 1.05 main arm, a directivity of -30 dB and coupling factor of -40 dB.
10. Receiver protectors through loss and reflection coefficients are assumed repeatable in low attenuation mode to an equivalent efficiency variation of 0.01 dB.

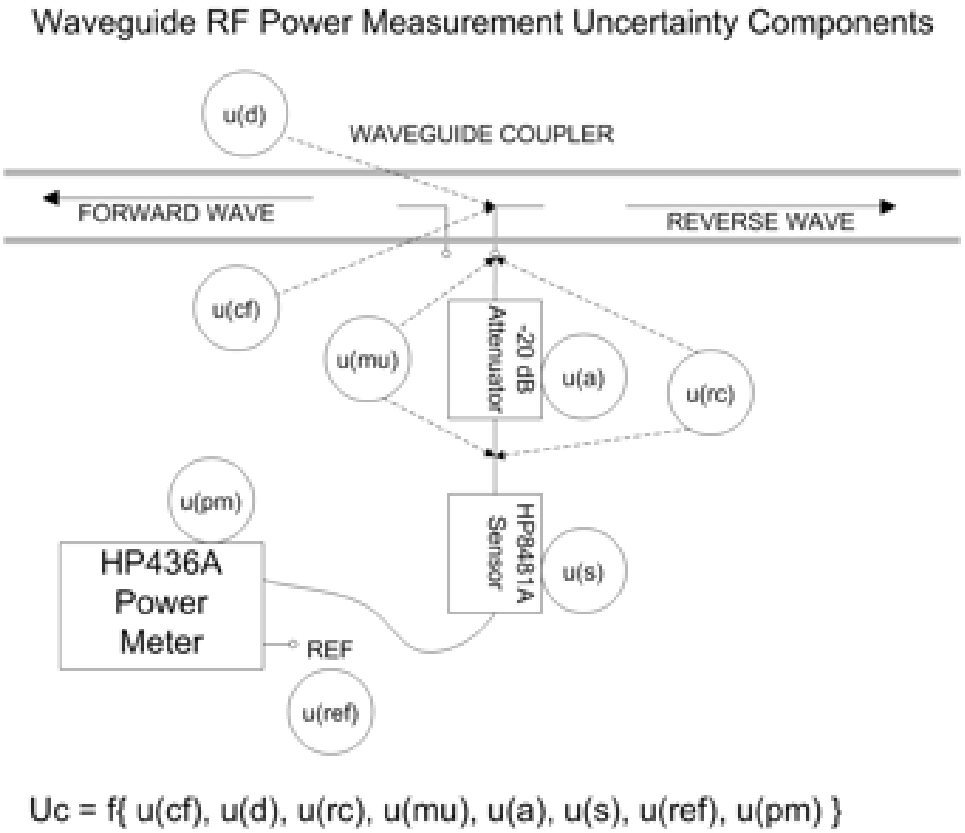

Figure 25: *For measuring directional microwave power inside a waveguide the following components are employed: waveguide coupler, precision attenuator, matched connectors, calibrated thermoelectric power sensor, calibrated power meter instrument, procedures, and recording of results. Errors at locations indicated by u(x) are broken out in the attached uncertainty budget.*

Example Uncertainty Budget: Practical Field Measurement of Waveguide Power

Test Conditions: Field Setting, -10C to 40 C, typical "good" VSWR limits, Power meter on optimum full-scale range; coupler with large coupling factor and high directivity. Maximum VSWR of power meter, attenuator ports, and coupler sidearm 1.1.

Uncertainty Components	Type	Limit	2-sigma %	2-sigma "dB"	N or U	1-sigma %	1-sigma^2 frac	Test or Measurement Conditions
Power Meter Instrument HP438A (bench), dB	B	0.042	0.972	0.042	N	0.486	2.361E-05	Bench conditions, individual measurements
Sensor HP8481A (bench), dB	B	0.092	2.141	0.092	N	1.070	1.146E-04	
Reference (Bench), dB	B	0.022	0.508	0.022	N	0.254	6.448E-06	
Square law deviations for modulations, dB	B	0.020	0.462	0.020	N	0.231	5.326E-06	
PM temperature uncertainty over 10C, dB	B	0.015	0.346	0.015	N	0.173	2.993E-06	u = -0.03 dB/10C*10C = 0.015dB
PM uncertainty over 0-90% RH, dB	B	0.050	1.158	0.050	N	0.579	3.352E-05	
Connector #1 repeatability (reference), dB	A	0.020	0.462	0.020	N	0.231	5.326E-06	
Connector #2 repeatability (mis), dB	A	0.000	0.000	0.000	N	0.000	0.000E+00	
Attenuator at 23C temp, dB	B	0.060	1.391	0.060	N	0.695	4.838E-05	
Attenuator temp uncertainty over 10C, dB	B	0.080	1.859	0.080	N	0.930	8.641E-05	u=10dB*10C*0.0004dB/dB/C=0.08
Attenuator heating	B	0.050	1.158	0.050	N	0.579	3.352E-05	u=20dB*0.005 dB/dB/W *0.5W=0.05dB
Waveguide coupler factor, dB	B	0.100	2.329	0.100	N	1.165	1.356E-04	
Waveguide coupler factor temps, dB	B	0.010	0.231	0.010	N	0.115	1.329E-06	u=0.0054dB/10C*20C=0.01dB
Directivity, dB	B	0.010	0.231	0.010	N	0.115	1.329E-06	
Short Test Cable attenuation variation, dB	A	0.020	0.462	0.020	N	0.231	5.326E-06	
Mismatch uncertainty of sidearm interface, dB	B	0.027	0.624	0.027	N	0.312	9.723E-06	
Connector #3 repeatability	A	0.020	0.462	0.020	N	0.231	5.326E-06	
Mismatch uncertainty of attenuator interface, dB	B	0.014	0.323	0.014	N	0.161	2.606E-06	
Connector #4 repeatability, dB	A	0.020	0.462	0.020	N	0.231	5.326E-06	
			0.000	0.000	N	0.000	1.000E-16	

Total	2.295E-02	uc % =	2.295
(all components)		uc (dB) =	0.099
		Coverage k	2.000
		Uk % =	**4.590**
		Uk (dB) =	**0.195**

Total Uncertainty under the defined and implied measurement conditions

Table B5: *Uncertainty budget for waveguide power measurement in circuit in the field, using typical test equipment and assuming good match conditions. The expanded uncertainty of microwave power measurement is estimated here at 0.2 dB for absolute power. Reducing the magnitude of selected components yields 0.11 dB for ratio measurements, and 0.05dB for ratios ignoring the coupling factor uncertainty.*

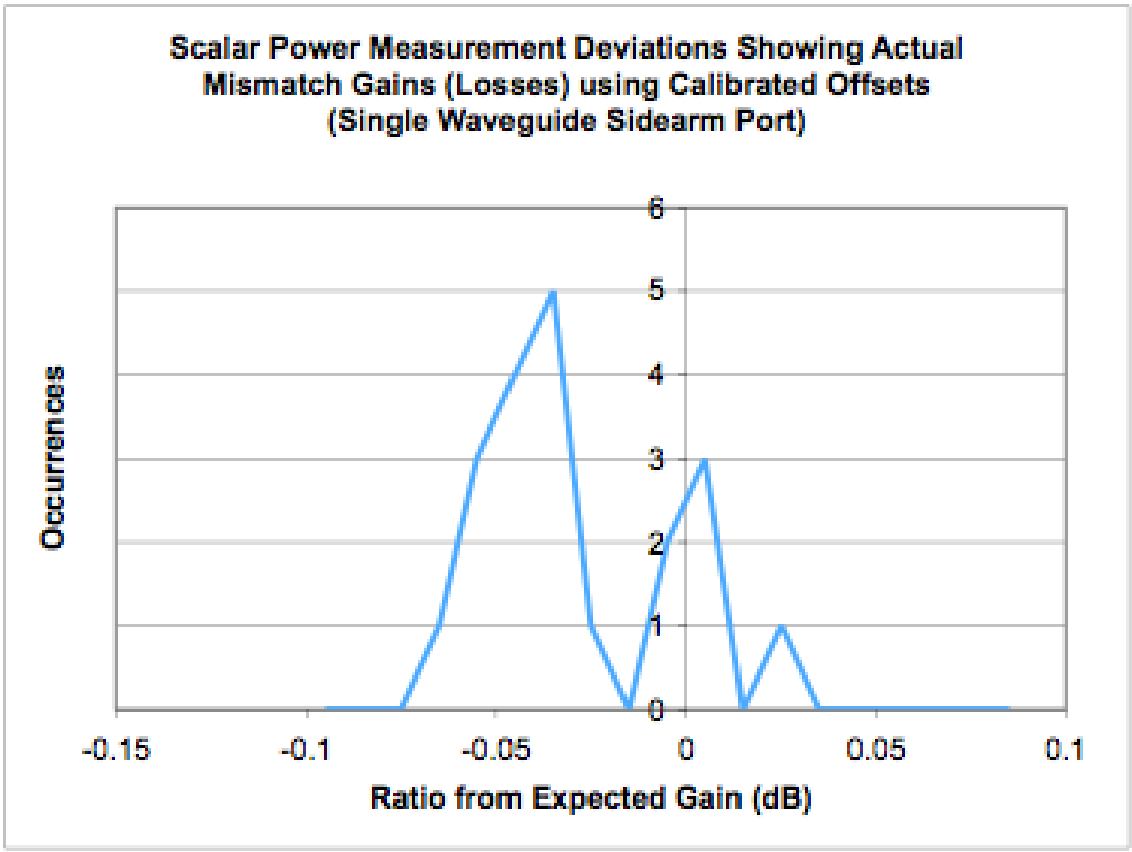

Figure 26: *Measured deviations from expected transmit power measurements using one or two identical calibrated offsets to alter the phase angle. Return loss was measured at approximately -20 dB for each side of the sidearm-attenuator interface of Figure 25*

.

11. Noise floor of a root-mean-square power measurement is assumed well behaved, uncorrelated, and subtracted from the composite signal to yield the power signal of interest.

12. Uncompensated receiver and digitizer non-linearities are less than 0.02 dB.

13. Receiver and digitizer drifts are less than 0.01dB over short intervals.

a) Uncertainty of Practical Waveguide Power Measurements – Experiments Two experiments have been conducted so far to provide preliminary evaluation of the uncertainty of waveguide power measurements. First, repeated power meter measurements were made using the configuration of Fig. 25 on a single waveguide coupler. One or two calibrated offsets 2.56 inches long were inserted between the waveguide sidearm and the attenuator to alter the effective phase angle. Phase of the calibrated offsets at 2800 MHz was approximately 160 degrees. Complex reflection coefficients of the sidearm and attenuator were measured with a vector network analyzer. As shown in Fig. 26 the deviation from expected path gain (loss) were numerically close to mismatch factors calculated as M_{gs} in Equation (13) above. Calculated mismatch factors were -0.056 dB for one phase offset and 0.019dB with two phase-offsets installed. Second, we attempted to obtain realistic experimental (Type A) standard uncertainty from scalar waveguide coupler ratio (differential) measurements of the type required in any EC approach. To randomize

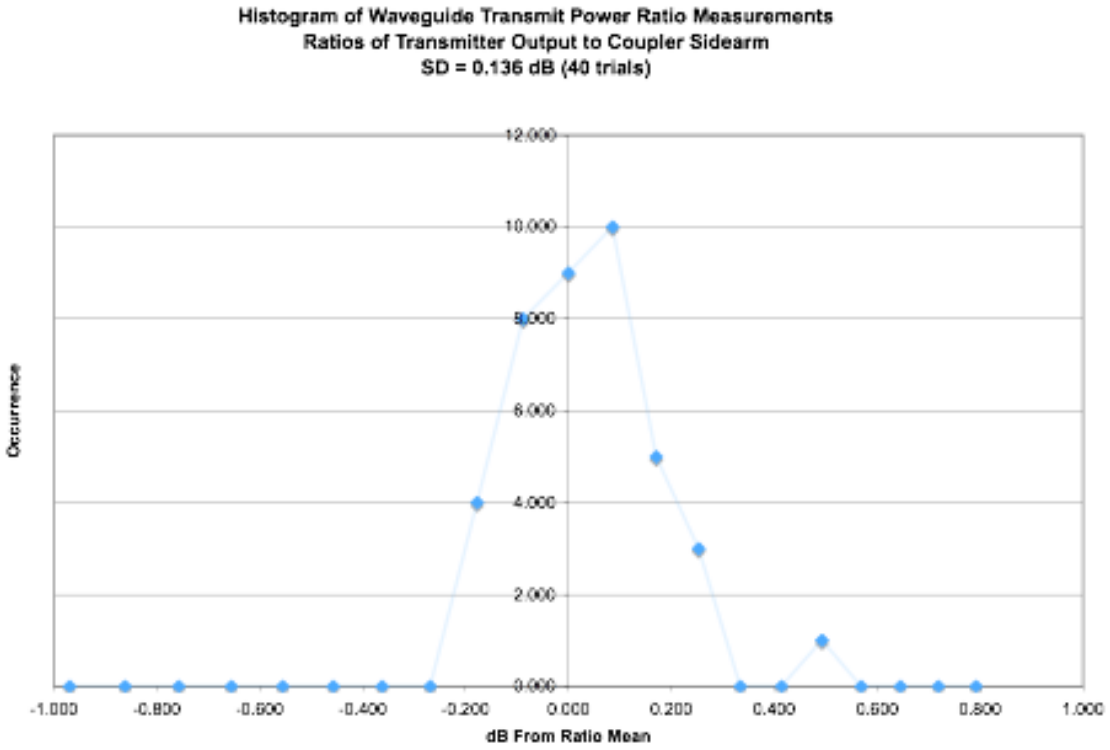

Figure 27: *Histogram of individual measurement deviations of a set of average transmit power measurements taken with randomized waveguide coupler sidearms, randomized attenuators, and randomized power sensors. Deviations in decibels from the ratio mean for an individual coupler are plotted on the x-axis.*

the trials, we employed three calibrated HP8481A power sensors, three "20 dB" precision attenuators, and two calibrated HP436A power meters selected at random, and then measured differential power from four coupler sidearms of identical make and model and possess directivity of -28 dB minimum. For each arm we abstracted the deviations after correcting for attenuator loss as measured with a vector network analyzer (VNA). The effective return loss of the coupler sidearms and the attenuators were less than -20 dB and return loss of power sensor less than -30 dB. The intention was to measure the practical effects of correcting for source stability, but not mismatch errors, reconnection errors, and other drift errors described above with Fig. 26 The design of this experiment omits coupling factor error. Other similar, but less complete, sets of transmitter power measurement data (not detailed here) provided sample standard deviations of between 0.075 dB and 0.128 dB from ratio mean.

b) Uncertainty of Practical Waveguide Power Measurements – Solar Flux Experiments The estimation of M_{bias} hinges on precise and well-understood far-field noise injection from the sun into the dual polarized antenna system. Solar source averaging and other corrections, such as deconvolving the source extent, may be applied to the on-sun measurements of noise power for the antenna far-field differential gain. As discussed in the main report, approximately 300 raster scans of the sun at 0.2-degree angular resolution were recorded at S-Pol between 14 June and 24 August 2006. The power ratio Hc/Vc was averaged from digitizer outputs, using over 300,000 independent samples near sun center. The repeatability of these ratios, as measured by the sample standard deviation, was approximately 0.025dB. Since

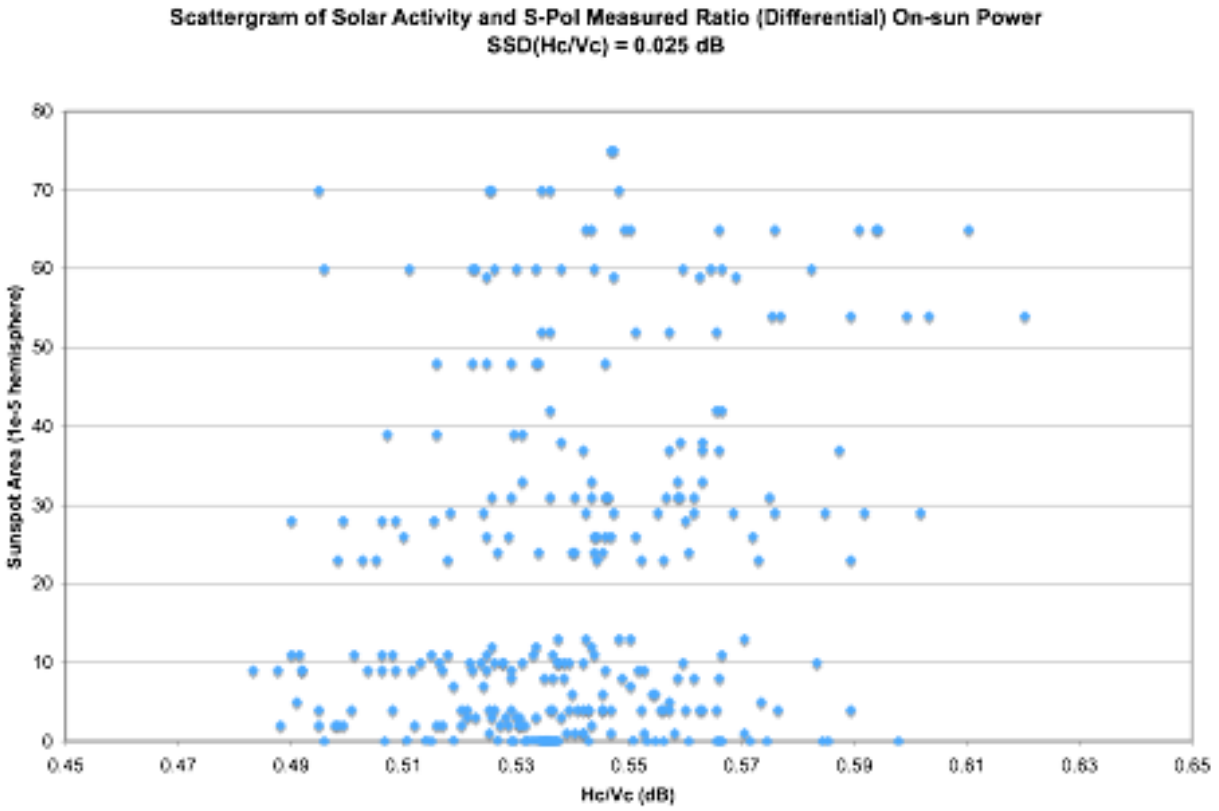

Figure 28: *Scattergram of NOAA SESC sunspot area plotted against measured solar power ratio. Digitizer readout from the S-Pol Hc copolar receiver and Vc copolar receiver were obtained from solar raster scan data. Fractional sample standard deviation relative to mean ratio was approximately 0.025 dB.*

the solar cycle is near minimum, when solar variability is unusually low, conclusions about the long-term repeatability of sun flux measurements should be taken with some caution. Solar flux at 10 cm during summer 2006 varied between 70 SFU to 90 SFU and sunspot area varied from zero to 75×10^{-5} fractional hemisphere. In the Figure 28, we see the desired result of little distinguishable correlation, however, more work may be needed here.

B.5 *Interim Recommendations for Engineering Calibration Approaches*

Power ratio calibration to the 0.1 dB uncertainty requires not only high quality equipment but also careful procedures. The following items are important to obtaining minimum variance calibration measurements. No priority is implied.

1. Insure that cables and connectors are clean, in protective storage, and replaced on schedule.
2. Precision attenuators with low VSWR are employed.
3. Waveguide couplers used for high quality scalar power measurements ideally have a -40 dB coupling factor, -30 dB directivity, and sidearm VSWR of 1.05 (return loss -30 dB).

4. Antenna and circulator return loss on H and V channels should be less than -20 dB and isolation between channels less than -30 dB.

5. Correct for source variations in transmitter, RF generator, and noise generator during measurements.

6. Check sidearm VSWR, power sensor, attenuator, splitters, and isolators in situ to insure conformance to specification.

7. Power splitters for injection ought possess excellent match and precisely measured power split.

8. Use of precision calibrated (fixed or sliding) offsets that alter the interface phase angle and thus minimize mismatch factor.

9. Use of isolators may be warranted.

10. Calibrate the ambient temperature performance of the power sensor used outside the laboratory.

11. Processing of digitizer readouts may need an external RF interference algorithm.

12. The ratio of H to V main beam solid angles, and main beam overlap, may be measured with a solar scan using appropriate processing.

13. Main beam solid angles and main beam overlap may contribute to Mbias (Z_{dr} measurement bias) for beam-filled targets in a way that may be measured.

14. Monitor sun for RF bursts at time of solar measurements (solar patrol).

15. Z_{dr} measurement bias recalibration should be conducted initially at frequent intervals to establish a control baseline for component degradation or replacement affecting subsequent calibrations.

16. All individual measurements and environmental data should be saved.

17. Certain staff seems more adept at making low-variance measurements.

18. Solar scans should be designed to minimize the effects of pedestal backlash, pedestal control variations, and background noise at the elevation angle of the sun.

19. Series adapters should not be employed, all measurable coaxial interfaces should be Type N.